

Insight on the Effect of Contour Height In Pressure Screening

by

Andreas Biniaris

B.A.Sc., The University of British Columbia, 2005

A THESIS SUBMITTED IN PARTIAL FULFILLMENT OF

THE REQUIREMENTS FOR THE DEGREE OF

MASTER OF APPLIED SCIENCE

in

THE FACULTY OF GRADUATE STUDIES

(CHEMICAL AND BIOLOGICAL ENGINEERING)

**THE UNIVERSITY OF BRITISH COLUMBIA
(Vancouver)**

April 2008

©Andreas Biniaris, 2008

ABSTRACT

The main purpose of this study is to determine the effect of contour height on the passage ratio of pulp through screen apertures, and determine which operating variable has the greatest affect on screen performance. In addition, a freeness model was to be developed to help predict the freeness change between accept and feed sides.

The study was conducted at The University of British Columbia (UBC) using a laboratory scale pressure screen. Slot velocity, feed consistency and contour height were the changing variables. Samples were collected from which passage ratio, freeness, fibre length and coarseness were determined.

From the studies conducted it was found that slot velocity had the greatest influence on the screen operation. As the slot velocity increased a greater force was applied to the fibre to help push it through the screen aperture. However, this increase in slot velocity decreases the fractionation ability (separation of fibres into different lengths) of the screen.

The second most important variable was the contour height. The main function of the contour height is to disrupt the flow of thick stock at the wall of the screen and allow for unhindered movement of fibre to the screen wall. The greater the contour height is, the greater the passage ratio (pulp fibre passing through screen). However, there is a decrease in fractionation.

The third most important factor was the feed consistency. At low feed consistencies there is less crowding in the screen. Less crowding leads to more loosely-formed flocs, which are easier for the contour height and the rotor to dissipate and thus leads to unhindered movement. Thicker feed stock has a negative effect on passage

A Freeness model was developed that showed that freeness had a power law relationship to passage ratio. The passage ratio was raised to a constant B, which is a function of the contour height and the feed consistency.

TABLE OF CONTENTS

ABSTRACT.....	ii
TABLE OF CONTENTS.....	iii
LIST OF TABLES.....	iv
LIST OF FIGURES.....	vi
ACKNOWLEDGEMENTS.....	viii
Chapter 1: Introduction.....	1
Chapter 2: Literature Review.....	6
2.1: Screening Theory.....	6
2.2: Passage Ratio.....	8
2.3: Screen and Rotor Hydrodynamics.....	10
2.3.1: Screen Hydrodynamics.....	10
2.3.2: Rotor Hydrodynamics.....	14
2.4: Screen Operating Parameters.....	14
2.5: Pulp Feed Furnish.....	16
Chapter 3: Experimental Procedure.....	17
3.1: Equipment and Material used.....	17
3.2: Experimental Procedure.....	18
3.3: Wet Lab Testing.....	19
Chapter 4: Results and Discussion.....	20
4.1: Effect of Contour Height on Passage.....	20
4.2: Effect of Feed Consistency on Passage.....	23
4.3: Effect of Contour Height on Accept Freeness.....	26
4.4: Effect of Feed Consistency on Accept Freeness.....	29
4.5: General Discussion.....	32
Chapter 5: Numerical Analysis.....	34
5.1: Dimensionless analysis.....	34
5.2: Equation for Passage Ratio.....	35
5.3: Equation for Accept Freeness.....	38
Chapter 6: Conclusion.....	40
Appendix A.....	42
Appendix B.....	44
Appendix C.....	50
Appendix D.....	56
Appendix E.....	67
Appendix F.....	76
Appendix G.....	79

LIST OF TABLES

Table 5.1: Results for Fitting Parameters equation.5.2.....	35
Table 5.2: Result for fitting parameters for equation 5.3 and R^2	36
Table 5.3: R^2 for fitting parameters in Table5.2 using equation 5.4.....	39
Table D.1: Experimental Data for 1.0% feed consistency and 0.6mm Contour Height.....	57
Table D.2: Experimental Data for 1.5% feed consistency and 0.6mm Contour Height.....	57
Table D.3: Experimental Data for 2.0% feed consistency and 0.6mm Contour Height.....	58
Table D.4: Experimental Data for 1.5% feed consistency and 0.6mm Contour Height.....	58
Table D.5: Experimental Data for 2.0% feed consistency and 0.6mm Contour Height.....	59
Table D.6: Experimental Data for 1.0% feed consistency and 0.9mm Contour Height.....	60
Table D.7: Experimental Data for 1.5% feed consistency and 0.9mm Contour Height.....	60
Table D.8: Experimental Data for 2.0% feed consistency and 0.9mm Contour Height.....	61
Table D.9: Experimental Data for 1.5% feed consistency and 0.9mm Contour Height.....	61
Table D.10: Experimental Data for 1.0% feed consistency and 0.9mm Contour Height.....	62
Table D.11: Experimental Data for 1.0% feed consistency and 1.2mm Contour Height.....	63
Table D.12: Experimental Data for 1.5% feed consistency and 1.2mm Contour Height.....	63
Table D.13: Experimental Data for 2.0% feed consistency and 1.2mm Contour Height.....	64

Table D.14: Experimental Data for 2.0% feed consistency and 1.2mm Contour Height.....	64
Table D.15: Experimental Data for 2.0% feed consistency and 1.2mm Contour Height.....	65
Table D.16: Experimental Data for 1.0% feed consistency and 1.2mm Contour Height.....	65
Table D.17: Experimental Data for 1.5% feed consistency and 1.2mm Contour Height.....	66
Table D.18: Experimental Data for 1.0% feed consistency and 1.2mm Contour Height.....	66
Table E.1: Passage Ratio Work Sheet for equation 5.2.....	67
Table E.2: Passage Ratio Work Sheet for equation 5.3.....	69
Table E.3: Accept Freeness Work Sheet for equation in figure 5.4.....	72
Table E.4: Comparison of Equation 5.4 with actual data.	74
Table G.1: Table G.1: Error analysis of fitting parameter B.	81

LIST OF FIGURES

Figure 1.1: Structure of Wood Chip (mech 401 notes).....	1
Figure 1.2: Pressure Screen Design.....	3
Figure 1.3: Typical Inner Surface Wedge Wire Design [13].....	3
Figure 2.1: Screen Variables [13].....	8
Figure 2.2: Contour plots of the turbulence kinetic energy near the screen surface for contour heights equal to (a) 0.3mm, (b) 0.6mm, (c) 0.9mm and (d) 1.2 mm [14].....	11
Figure 2.3: Fluid streamlines at the aperture entry for contour heights equal to (a) 0.3mm, (b) 0.6mm, (c) 0.9mm and (d) 1.2mm for a 3.2mm wide wire showing how the vortex size and location vary. [14].....	11
Figure 2.4: Contour plots of the turbulence kinetic energy near the screen surface for wire width equal to (a) 2.6mm, (b) 3.2mm (c) 4.0mm [14].....	13
Figure 2.5: Fluid streamlines at the aperture entry for Wire width (a) 2.6mm, (b) 3.2mm, (c) 4.0mm [14].....	13
Figure 3.1: UBC G&LV/ Beloit model MR-8 screening equipment.....	17
Figure 3.2: AFT Foil Rotor.....	18
Figure 4.1: Passage Ratio vs. Slot Velocity 0.6mm contour height.....	20
Figure 4.2: Passage Ratio vs. Slot Velocity 0.9mm contour height.....	21
Figure 4.3: Passage Ratio vs. Slot Velocity 1.2mm contour height.....	22
Figure 4.4: Passage Ratio vs. Slot Velocity 1.0% feed consistency.....	23
Figure 4.5: Passage Ratio vs. Slot Velocity 1.5% feed consistency.....	24
Figure 4.6: Passage Ratio vs. Slot Velocity 2.0% feed consistency.....	25
Figure 4.7: Accept Freeness vs. Slot Velocity 0.6mm contour height.....	26
Figure 4.8: Accept Freeness vs. Slot Velocity 0.9mm contour height.....	27
Figure 4.9: Accept Freeness vs. Slot Velocity 1.2mm contour height.....	28

Figure 4.10: Accept Freeness vs. Slot Velocity 1.0% feed consistency.....	29
Figure 4.11: Accept Freeness vs. Slot Velocity 1.5% feed consistency.....	30
Figure 4.12: Accept Freeness vs. Slot Velocity 2.0% feed consistency.....	31
Figure 5.1: Fitting parameter B variation with consistency and contour height.....	36
Figure 5.2: Experimental Passage vs. Calculated Passage Ratio.....	37
Figure 5.3: Plot of Freeness vs. Passage ratio.....	38
Figure 5.4: Experimental Freeness vs. Calculated Freeness.....	39
Figure B.1: Accept Fibre Length 0.6mm Contour Height.....	44
Figure B.2: Accept Fibre Length 0.9mm Contour Height.....	45
Figure B.3: Accept Fibre Length 1.2mm Contour Height.....	46
Figure B.4: Accept Fibre Length for 1.0% feed Consistency.....	47
Figure B.5: Accept Fibre Length for 1.5% feed Consistency.....	48
Figure B.6: Accept Fibre Length for 2.0% feed Consistency.....	49
Figure C.1: Accept Coarseness vs. Slot Velocity 0.6mm Contour height. FQA Error Bar=0.005.....	50
Figure C.2: Accept Coarseness vs. Slot Velocity 0.9mm Contour height.....	51
Figure C.3: Accept Coarseness vs. Slot Velocity 1.2mm Contour height Experimental Error Bars= 95% Confidence.....	52
Figure C.4: Accept Coarseness vs. Slot Velocity 1.0% Feed Consistency.....	53
Figure C.5: Accept Coarseness vs. Slot Velocity 1.5% Feed Consistency.....	54
Figure C.6: Accept Coarseness vs. Slot Velocity 2.0% Feed Consistency.....	55

ACKNOWLEDGEMENTS

I would like to start off by thanking my supervisors Mark Martinez and James Olson. Their insight and support was of great value in completing this project. Also, many thanks go out to the PPC grad students who were always willing to help me out when I got stuck on a problem. Thanks to Tim Paterson for maintaining the mechanical aspects of the machine and for always fixing any problems I encountered.

I would like to thank my family and friends for their continual assistance during my time in the masters program, and their help in many different aspects. Their continual support has always given me strength.

Finally I would like to express my sincere appreciation to Vivian Heish for taking so much of her time and helping me edit this thesis. One day I hope to return the same level of assistance that she gave me.

If A is success in life, then A equals x plus y plus z.
Work is x; y is play; and z is keeping your mouth shut.
Albert Einstein

It does not matter how slowly you go so long as you do not stop.
Confucius

CHAPTER 1: INTRODUCTION

Pulping is the process in which wood chips, or other non-wood products, are broken down into their individual fibres. There are a number of ways to accomplish this, one being chemical pulping and another being mechanical pulping. The final products of these processes have a number of uses, including paper making, to cardboard containers.

The primary feed stock for the pulping process comes from wood. Two different types of wood are used: hardwood and softwood. Hardwood trees have shorter fibre length and are generally used for paper grades that require bulk and smoothness. Softwood trees have a longer fibre length and resemble cylindrical tubes; they are generally used for making grades that require high strengths. As seen in Figure 1.1 there are many fibres in a wood chip and they are held together by lignin, the material that is located in the middle lamella.

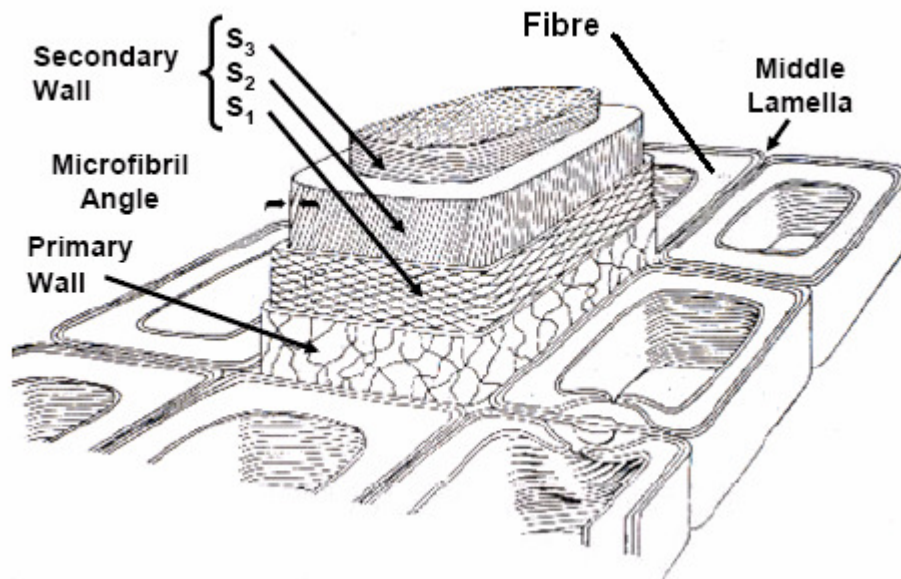


Figure 1.1: Structure of wood chip. [18]

As stated earlier the purpose of pulping is to break down the wood chip into its individual fibre structure. Chemical pulping does this by using a chemical mixture of sodium hydroxide (NaOH) and sodium sulfide (Na₂S) called white liquor to break down the lignin and only some of the hemicellulose leaving mostly cellulose. This is done in a high temperature high pressure unit called a digester. Some variations of mechanical pulping use chemicals; however, the main principle is to introduce a large amount of mechanical work to the chip. This is done through units called refiners, which consist of two large disks. There are a number of configurations for refiners. Two possible configurations: both disks spinning or one spinning and one stationary. When the chip moves into the refining zone, it is torn into individual fibres. However, both chemical and mechanical pulping processes leave undesirable material in the product.

Undesirable materials include shives and dirt. Shives are bundles of fibres that have not been separated during processing. Both mechanical and chemical processes produce shives, though the amount produced is small in comparison to the overall flow. Even though these impurities are in small quantities, they reduce the strength and optical properties of paper. The most commonly used industrial process to remove these contaminants is pressure screening.

Pressure screens have the ability to separate undesirable material based on the size of the contaminant. This allows for the separation of fibres that require more refining from the well-processed ones. Figure 1.2 shows that there are two main components to the screen: the screen basket and the rotor.

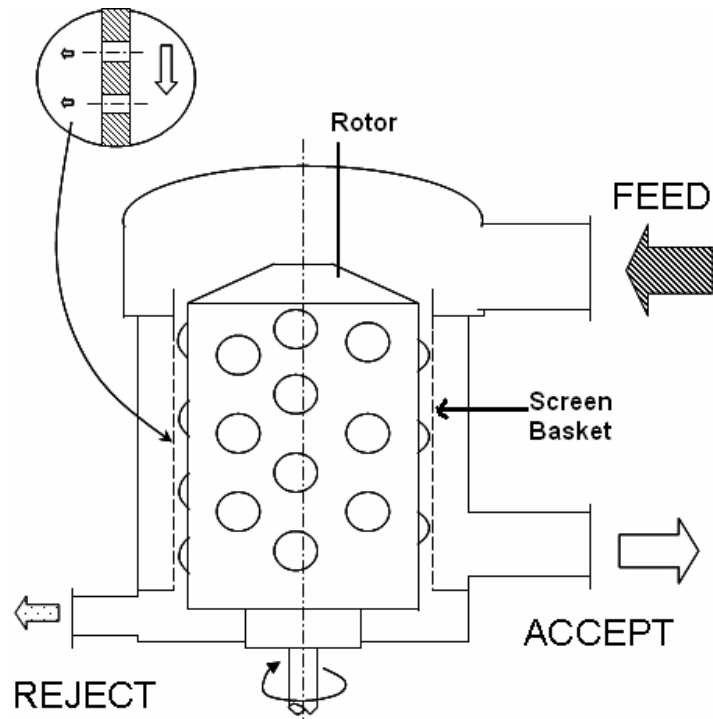


Figure 1.2: Pressure Screen Design.

There are a number of screen basket designs, ranging from drilled holes to slotted screens. Newer designs use a wire wedge which allows for larger open area slotted screens. These screen baskets act as barriers and have the ability to create flow fields that limit the passage of contaminants through the screen opening into the accept stream. These flow fields are created by the inner surface of the screen. Figure 1.3 shows the main geometry of the inner surface of a wire wedge screen basket.

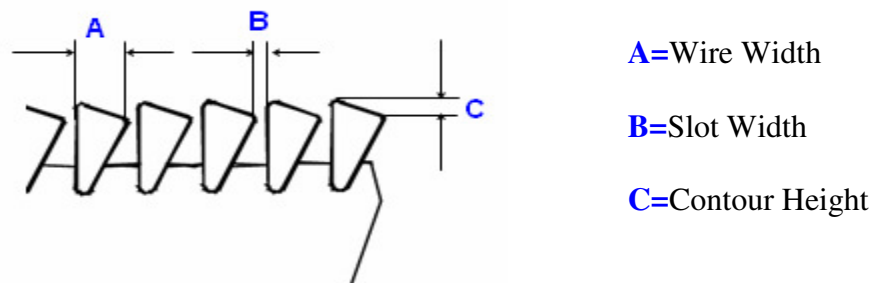


Figure 1.3: Typical Inner Surface Wedge Wire Design [14]

The second major piece of equipment in the pressure screen system is the rotor. The main purpose of the rotor is to induce a tangential fluid flow over the screen surface to increase the turbulence (assist in disruption of flocs) of the system. In addition, it causes a pressure pulse which first creates a positive pulse that helps push fibres through and then a negative pulse that helps back flush the apertures of the screen. There are many different styles of rotors, ranging from solid core to foils. Solid cores are mostly used in high consistency screening, whereas foils are used at lower consistencies.

This thesis focuses on studying how screen geometry and certain operating conditions affect the performance of the screen. Specifically, the study will focus on the effect of the screen contour height, the feed consistency and the slot velocity. The testing will be completed on a laboratory scale pressure screen using AFT (Advance Fibre Technologies) macro flow screen baskets. The fibre furnish used will be Chemical Thermal Mechanical Pulp supplied from Quesnel River Pulp Company. Accept and reject samples will be collected from the screen at pre-determined operating conditions, stated in Chapter 3. From samples collected, the passage ratio, freeness, fibre length, coarseness will be determined. From this data, factors that play a major role in the screening operation will be determined, and a freeness model will be developed. Freeness is one of the most important properties to pulp and paper makers. Having freeness model will help better determine freeness changes across a screen, allowing for better control.

The first section of the thesis consists of a literature review (Chapter 2). This will include a general discussion about the theory behind screening. In addition it will review major

studies already completed. These studies focus largely on screen operating conditions as well as the basket geometry.

In Chapter 3, the experimental equipment will be covered in detail. In addition, the exact experimental conditions tested and laboratory procedures used will be described.

In Chapter 4 results are presented and discussed. The first set of results will be the passage ratio for the different screens. This is an important factor when looking at the capacity of the screen. Next set of results will be the freeness (CSF). This variable is very important in pulp industry since it gives an estimate to the draining ability of pulp, which is important factor when operating paper machines. The final two factors looked at are the fibre length and the fibre coarseness. These play large factors in paper properties

In Chapter 5, a numerical analysis is completed. The purpose is to determine a relationship between accept freeness and passage ratio. The excel spread sheets are shown in Appendix E.

Finally, in Chapter 6 conclusions will be drawn on which variables, studied, had the largest effect.

CHAPTER 2: LITERATURE REVIEW

2.1 Screening theory

When looking at pressure screening there are two primary methods of separation: barrier and probability screening. In barrier screening contaminants cannot fit through the screen since the size of the contaminant is much larger than the aperture size. In probability screening at least one dimension of the contaminant is able to pass through the aperture, so depending on factors which orientate the fibre there is a chance for the contaminant passing through [9]. Two common Efficiency-Reject rate curves used were presented by Nelson 1981, eqn: 2.1 and by Kubat & Steenberg 1955, eqn: 2.2

$$E_R = \frac{R}{1 - \alpha + \alpha R}$$

E_R = Removal Efficiency
 R = Mass Reject (Eqn: 2.1)

$$\alpha = \text{Screening Quotient} = 1 - \frac{\text{Passage Ratio Contaminants}}{\text{Passage Ratio Pulp}}$$

$$E_R = R^\beta$$

E_R = Removal Efficiency
 R = Mass Reject (Eqn: 2.2)

$$\beta = \text{Screening Index} = \frac{\text{Passage Ratio Contaminants}}{\text{Passage Ratio Pulp}}$$

Equations 2.1 and 2.2 were widely used in screening operations; however, their derivations were not well documented and as such the equation were not completely understood. In 1989 [7] Goodings and Kerekes derived eqn 2.1 using a perfect mixing case adjacent the screen plate, while eqn 2.2 represents a plug flow model in this zone [15]. In their analysis they found that both the Screening Quotient and Screening Index

were functions of the pulp and contaminant passage ratios (Passage ratio is defined by equation 2.5). However, these original equations (eqn 2.1 and 2.2) do not include the effect of barrier screening. The E-R curves were determined again this time by applying the effect of barrier screening. These equations are shown below.

$$E_R = \frac{R}{1 - \alpha + \alpha R} \left(1 - \frac{C_{f \cdot \alpha \cdot \delta \alpha r}}{C_{f \cdot c}} \right) + \frac{C_{f \cdot \alpha \cdot \delta \alpha r}}{C_{f \cdot c}}$$

E_R = Removal Efficiency
 R = Mass Reject (Eqn: 2.3)
 α = Screening Quotient
 $C_{f \cdot \alpha \cdot \delta \alpha r}$ = Concentration Contaminants Removed by Barrier
 $C_{f \cdot c}$ = Concentration Contaminants In Feed

$$E_R = R^\beta \left(1 - \frac{C_{f \cdot \alpha \cdot \delta \alpha r}}{C_{f \cdot c}} \right) + \frac{C_{f \cdot \alpha \cdot \delta \alpha r}}{C_{f \cdot c}}$$

E_R = Removal Efficiency
 R = Mass Reject (Eqn: 2.4)
 β = Screening Index
 $C_{f \cdot \alpha \cdot \delta \alpha r}$ = Concentration Contaminants Removed by Barrier
 $C_{f \cdot c}$ = Concentration Contaminants In Feed

These equations show that screening efficiency increases as reject rate is increased. They also show that efficiency is related to the pulp and contaminant passage ratios. The passage of pulp however depends on a number of factors.

2.2 Passage Ratio

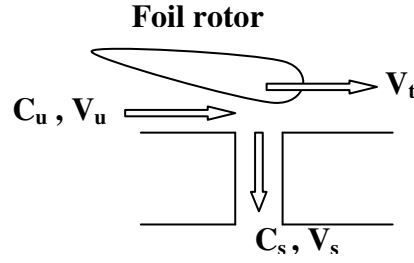


Figure 2.1: Screen Variables [15]

The passage ratio, can be defined in terms of pulp passage (P_p) or contaminant passage (P_c), is defined as the consistency, pulp or contaminants, in the flow through the screen aperture (C_s), divided by the consistency, pulp or contaminants, in the flow immediately up-stream of the aperture (C_u):

$$P = \frac{C_s}{C_u} \quad . \quad (\text{Eqn: 2.5})$$

By applying a plug flow analysis it can be found that the passage ratio is based on the volumetric reject ratio R_v and the thickening factor T .

$$P = \frac{\ln(T)}{\ln(R_v)} + 1 \quad (\text{Eqn: 2.6})$$

Volumetric reject ratio is defined as the flow rate of reject over the flow rate of the feed, (Q_r/Q_f) and the thickening factor is defined as the concentration of the reject over the feed (C_r/C_f). When applying the mixed model analysis the passage ratio was determined to be

$$P = \left(\frac{1}{T} - R_v \right) \left(\frac{1}{1 - R_v} \right). \quad (\text{Eqn: 2.7})$$

When comparing the two models to actual screen data it was found that the plug flow model is more accurate [13]. It was found that the passage ratio was governed by two factors: a “wall effect” and a “turning effect” [15]. The wall effect showed that the fibre that passes into the aperture comes from a layer close to and oriented nearly parallel to the surface of the screen [6]. The concentration of pulp in the “exit layer” was also found to be less than that in the bulk stream. For the fibre to enter the aperture it has to rotate 90 degrees. Because of this, more flexible fibres are accepted due to the ability of following fluid streamlines. This is known as the turning effect. It was later suggested that this turning effect was a function of fibre penetration, rotation and bending [14]. Other factors that are found to influence the passage of fibre are stapling and plugging of apertures [14]. Staples occur when a fibre get stuck on the surface of the screen and is neither rejected nor accepted. Staples can be vertical or horizontal and the mode is governed mainly by the V_s/V_u (slot velocity and upstream velocity, respectively).

In recent studies the effect of feed furnishes on screening was determined [9]. It was found that the longer the feed fibre length the greater the decrease in passage ratio. This was most likely caused by the increase in fibre-fibre interactions, which hinders the movement and the passage of individual fibres through the screen apertures. The degree of fractionation was also found to depend on the arithmetic fibre length distribution. When the fibre distribution curves were found to be thin, then there was not a large difference between accepts and rejects distribution. However, when there was a wide distribution in length it was found that there was a larger degree of separation between the fractions between accepts and the rejects [9].

2.3 Screen and Rotor Hydrodynamics

Mechanical factors affecting screening include screen geometry and rotor design. There is a wide variety of screen styles, ranging from holed to slotted. Slotted screens have become increasingly popular since they allow for a screen slot width of 0.1mm, without the loss of capacity. As shown in Figure 1.3 there are 3 main screen geometries: the contour height, the wire width and the slot width.

2.3.1 Screen Hydrodynamics

Contour height is a measurement of the surface roughness of the screen. There are 3 purposes to the contour height. The first is to redirect the tangential flow into the apertures and facilitate the passage of fibres. The second is to reduce the hydraulic resistance of flow that turns into the slot. Thirdly, counter height creates turbulence at the screen surface which fluidizes the fibre suspension [17]. Studies conducted by Dong et al., using CFD software, showed that a sloped slot entry had better performance than a smooth or a stepped surface [4]. Recently, CFD models of contoured screens were developed by Mokamati et al [17] that showed that a larger contour height put larger amount of energy into fibre suspension that helps break up flocs and allows for passage of fibres. These results are shown in Figure 2.2 below. In Figure 2.3 the increase in vortex size due to contour height is seen. Also seen is how the center of this vortex shifts away from the slot.

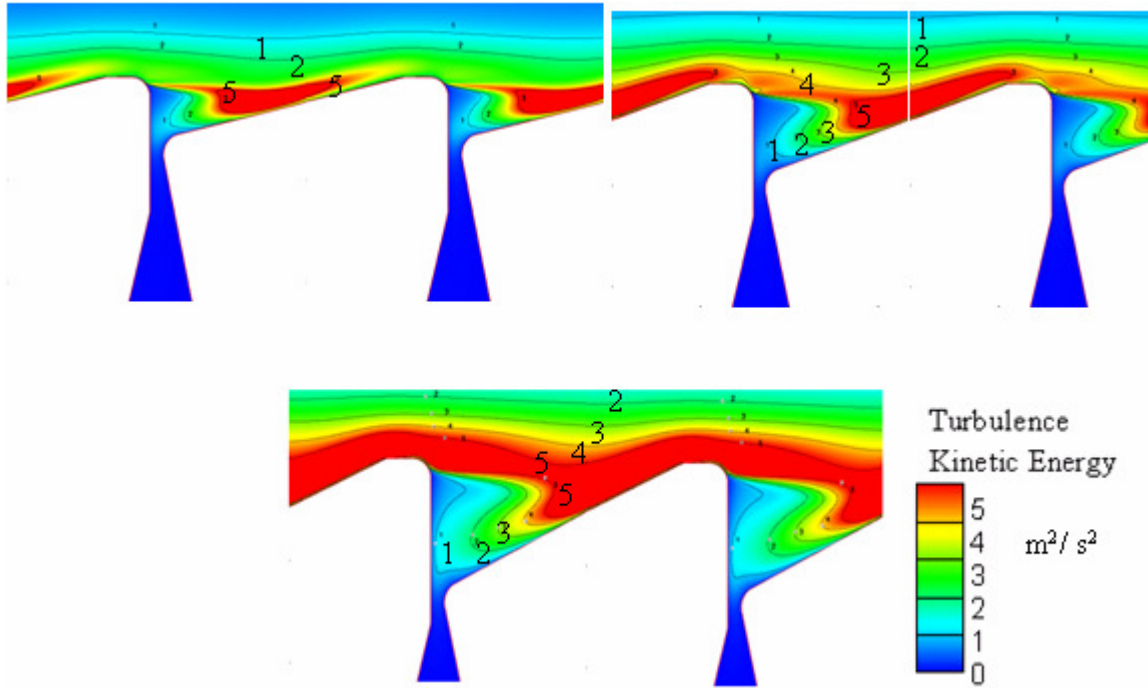


Figure 2.2: Contour plots of the turbulence kinetic energy near the screen surface for contour heights equal to (a) 0.3mm, (b) 0.6mm, (c) 0.9mm and (d) 1.2 mm [17]

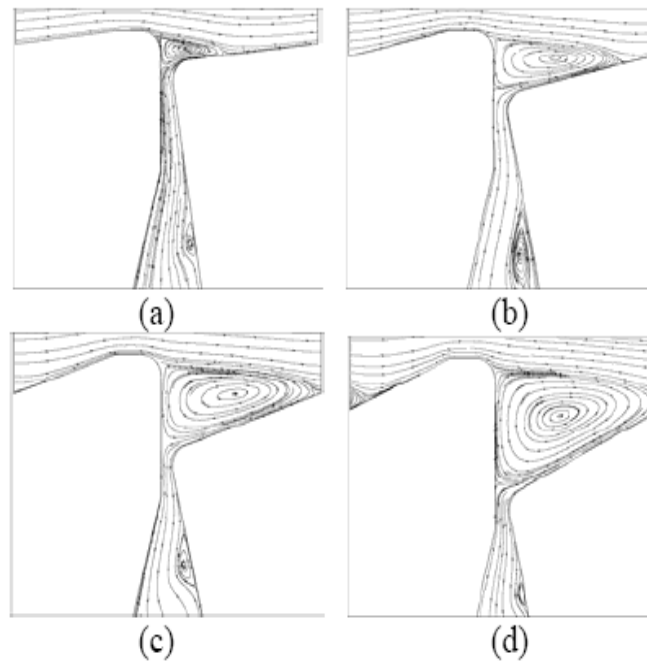


Figure 2.3: Fluid streamlines at the aperture entry for contour heights equal to (a) 0.3mm, (b) 0.6mm, (c) 0.9mm and (d) 1.2mm for a 3.2mm wide wire [17]

Experiments conducted by Jokinen et al. [11] found an increase in capacity with an increase in contour height. It was concluded, that the increase in turbulence at the screen wall was the primary cause of this. The study conducted by Saurabh Kumar, on the removal efficiency of stickies from pulp [16], found that increase in contour height lead to better fractionation but a decrease in removal efficiency. The best stickies removal was found at lower contour heights [16]. However, findings by Ari Ammala show that fractionation decreases with increasing contour height. He suggested that there is a limit to the contour height, at which no significant changes in fractionation occurs [2].

Studies conducted on wire width [10, 11, 14] have found that decreasing the wire width does not necessarily increase the capacity of the screen. The flow vortices were seen to stretch and move further away from the screen aperture as width increase, shown in Figure 2.5. It is also seen that the turbulent kinetic energy decreases as the wire width increases, Figure 2.4 [17]. Decreasing the wire width can also lead to a stapling effect in which a fibre tries to enter two apertures at the same time. This will lead to a loss of capacity. However, Jokinen et al. suggests that the decrease in capacity could be caused by the increased flow disturbance at the inlet and outlet of the slot [11].

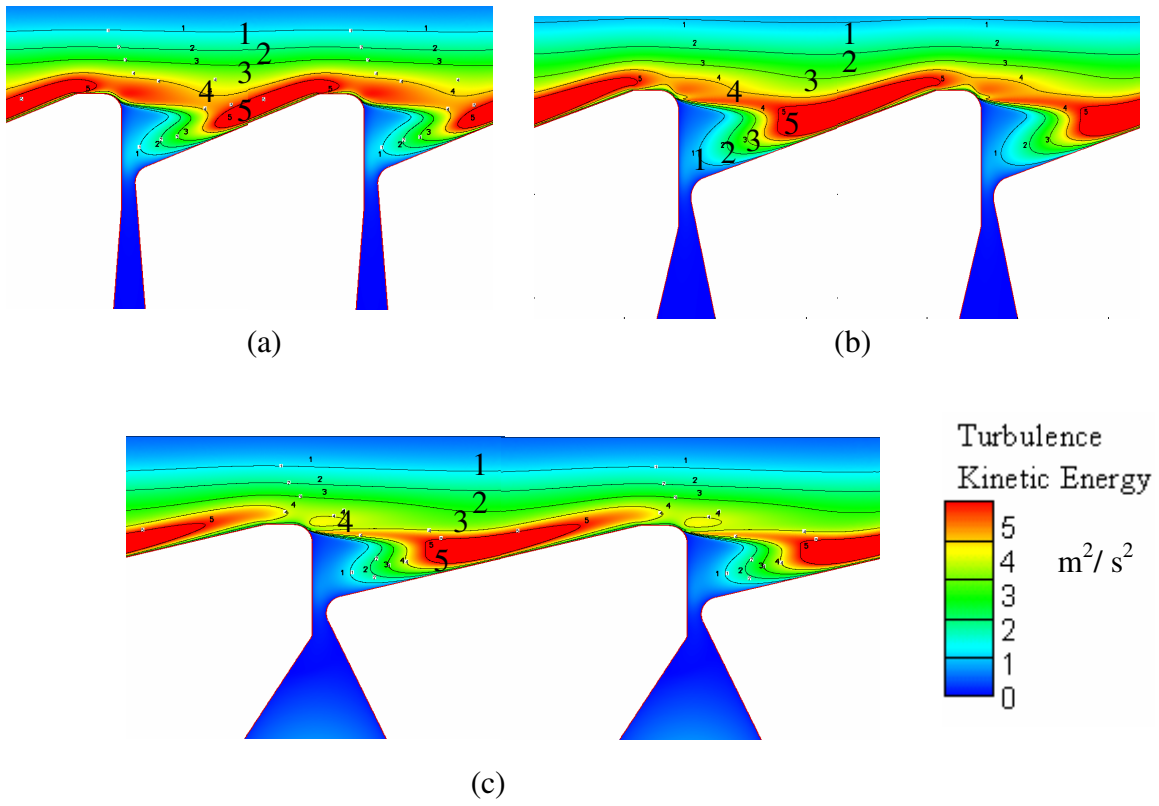


Figure 2.4: Contour plots of the turbulence kinetic energy near the screen surface for wire width equal to (a) 2.6mm, (b) 3.2mm (c) 4.0mm [17]

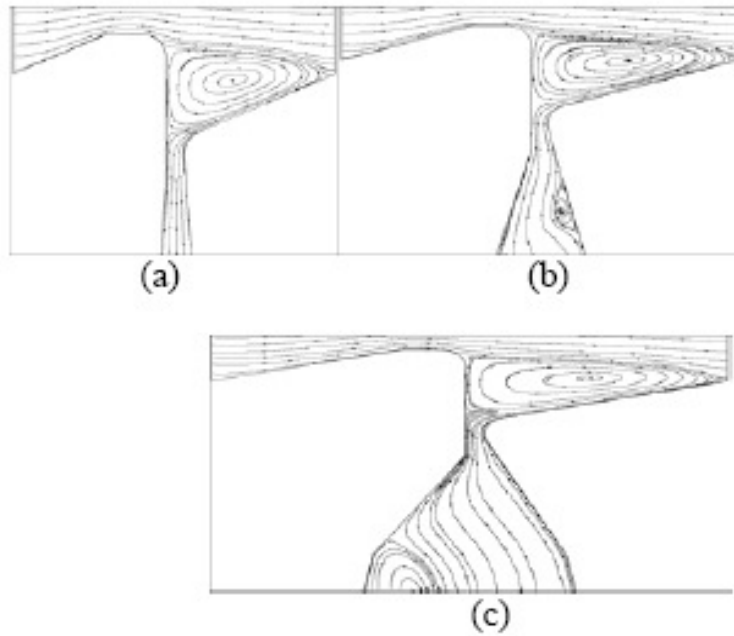


Figure 2.5: Fluid streamlines at the aperture entry for Wire width (a) 2.6mm, (b) 3.2mm, (c) 4.0mm [17]

The slot width has a direct affect on the capacity of the screen basket. Jokinen et al [9, 10] found that increasing the slot width decreases the hydraulic resistance and increase the capacity; however, this leads to a decrease in the removal efficiency.

2.3.2 Rotor Hydrodynamics

The function of a rotor is to keep the screen free from debris particles while “fluidizing” the pulp suspension. It accelerates the pulp suspension in the screen basket and to allow for a higher tangential velocity. Another and more important function is to create a negative pressure pulse that cleans and prevent the plugging of screen apertures. Styles of rotors range from foil rotors for low consistency screening and solid core rotor, which are used for high consistency screening [13]. Studies have shown that high tip speeds decrease selectivity (between short and long fibres) but increase the passage ratio [21, 12]. Other research is focused on multi element foils. It was found that the pressure pulse can be controlled; decrease in forward pulse and an increase in the back flushing pulse. In addition to being able to control pulse shape, the energy requirements decrease [20].

2.4 Screening Operating Parameters

When looking at screening, there are a limited number of variables that can be controlled. These variables include reject ratio, slot velocity, and tip speed. As stated before the reject ratio is defined as the reject flow over feed flow. Small volumetric reject rates will

increase the fractionation selectivity, but operating a pressure screen at a small volumetric reject is difficult because of high reject thickening, which might lead to screen blinding (fibre buildup on the feed side of the screen) [8]. Studies also show the volumetric reject ratio that provides the optimal fractionation efficiency depends on fibre passage ratio, and in turn on slot width and slot velocity [19].

Another important variable is the slot velocity which is defined as the velocity at which the fluid is exiting the slots of the screen basket. The slot velocity is defined as the accept flowrate divided by the open area of the screen. An increase in slot velocity is reported to reduce screening efficiency [16], especially if the debris is compressible, as is the case with stickies; however, fibre passage ratio increases. The method in which the passage ratio changes with slot velocity is dependent on fibre length [15, 14]. The effect of slot velocity was found to be equivalent to the effect as slot width [19].

The final controlled parameter is the rotor tip speed. An increase in the tip speed leads to an increase in the strength and frequency of pulsations. Higher foil tip speed will increase the capacity and reduce the screening efficiency [8]. The reason for the increase in passage is because of the increase in upstream velocity. Gooding's [5] determined that the upstream velocity is a function of the axial flow and the tip speed. The effects of tip speed are noticed more when dealing with contour heights. This is based on increasing turbulence and fluidization of the pulp suspension, which is thought to reduce the flow resistance over the screen plate [2]. Energy consumption is related almost entirely to rotor frequency [2], the frequency required being dependent on the network strength of the fibre suspension and the desired accept capacity.

2.5 Feed Pulp Furnish

Another major factor in screening is the quality of the pulp that is being screened. Studies show that pH, temperature and viscosity have major effects [2]. Increasing pH and temperature leads to an increase in the capacity of the screen. The reason for the pH has this effect is because alkaline acts as a lubricant which assists with the passage. Temperature has also shown to improve passage due to an increase in fibre flexibility [1], but also leads to a decrease in the screening efficiency, caused by contaminants becoming malleable [2]. The increase in capacity due to viscosity is attributed to the decrease in the ability to re-flocculate because of the increase in the viscosity.

CHAPTER 3: EQUIPMENT AND PROCEDURE

3.1 Equipment & Material Used

The work for this thesis was completed on a G&LV/ Beloit model MR-8 (Figure 3.1). The system is fully automated and controlled using LAB View. The system includes pneumatic control valves, magnetic flow meters and pressure transducers on the main flow lines. This allows the quick and accurate collection of data which is saved on to the operating computer. The pump is operated using a Variable Frequency Drive (VFD) which allows the operation at any number of inlet conditions. In addition to the pump, the rotor motor is also attached to a VFD which allows the testing of any tip speed desired and returns accurate power reading for the rotor

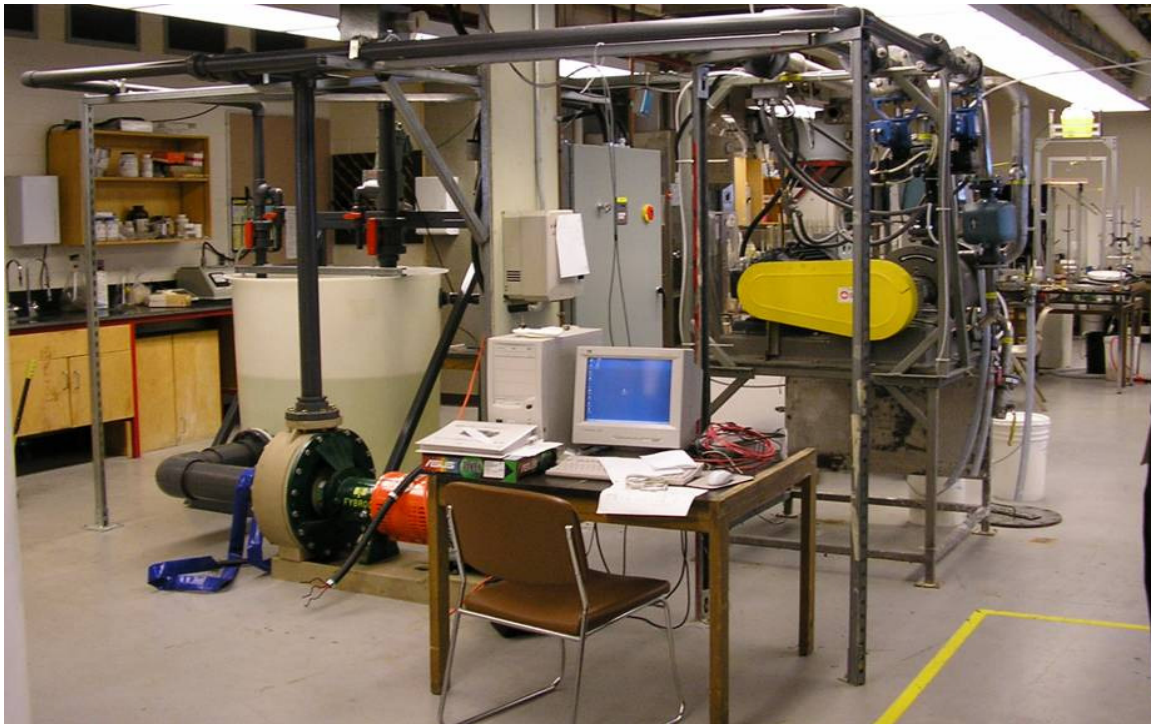


Figure 3.1: UBC G&LV/ Beloit model MR-8 screening equipment.

The rotor used was an Advance Fibre Technologies (AFT) foil rotor (Figure.9) and the screen baskets were AFT Macro-Flow. Three contour heights chosen to look at were 0.6mm, 0.9mm and 1.2 mm. The wire width was kept constant at 3.2mm and the slot width was also constant at 0.15mm. Feed Pulp was CTMP from Quesnel River Pulp (quality sheet in Appendix F).



Figure 3.2: Advance Fibre Technologies Foil Rotor

3.2 Experimental Procedure

The first step, in setting up a run, was to clean the machine from old pulp. Clean water was running through the system until old fibres were no longer present. If need be the screen housing would be opened and the screen basket would be changed. The dry pulp would be loaded into the tank and then filled with hot water. Immersible heaters were turned on and the pulp was mixed for twelve hours before a run was conducted. This procedure would ensure proper re-pulping and latency removal. At the time of the test the pulp temperature was 50° Celsius.

The tests were run at a constant volumetric reject (R_v) of 0.25 and the tip speed was set to 17m/s. The slot velocity was varied from 0.5m/s to 3m/s. During operation, accept and reject valves were manipulated until the desired flow rate was attained. The sample ports were opened and the flow was allowed to stabilize; after which, one liter samples were

collected from the accept line and the reject line. Feed samples were collected at a slot velocity of 0.5 and 1.5 m/s. Each trial would take an hour and it was found that there was no variation in the feed properties. Rotor power readings were taken as well as pressure reading for each stream. To check the repeatability of the tests a single test condition was chosen and run multiple times.

3.3 Wet Lab Testing

Pulp properties that were determined were the consistency, freeness, fibre length and coarseness. For the consistency measurement roughly 100 grams of each sample was filtered using Whatman Qualitative Filter Paper, 4th grade. The samples were then dried in an oven to determine the dry fibre weight. The dry fibre weight divided by the total weight gives the consistency as a mass fraction. The freeness was determined using the Canadian Standard Freeness (CSF) tester. From the sample beakers 3 grams of dry fibre was weighed out and then diluted to one liter. The solution was then loaded into the drainer and then allowed to drain. The freeness test was conducted until two tests were within five milliliters of each. To determine the fibre length and coarseness, a Fibre Quality Analyzer (FQA) was used. The first step is to prepare 2 gram handsheets which were allowed to stabilize in a CTH (Constant Temperature Humidity) room. Once the handsheets were stabilized 30mg oven dried fibre was torn into 200ml flasks and filled with distilled water. These flasks were allowed to soak over night and then were shaken until the fibres are separated. They are transferred into beakers, then filled up with 4 liters of distilled water and well stirred. The FQA containers are filled with solution, one with 600ml of solution, for the coarseness and one with 500ml, for the fibre length. To test the accuracy of the FQA one test condition was run multiple times.

CHAPTER 4: RESULTS & DISCUSSION

4.1 Effect of Contour Height on Passage Ratio.

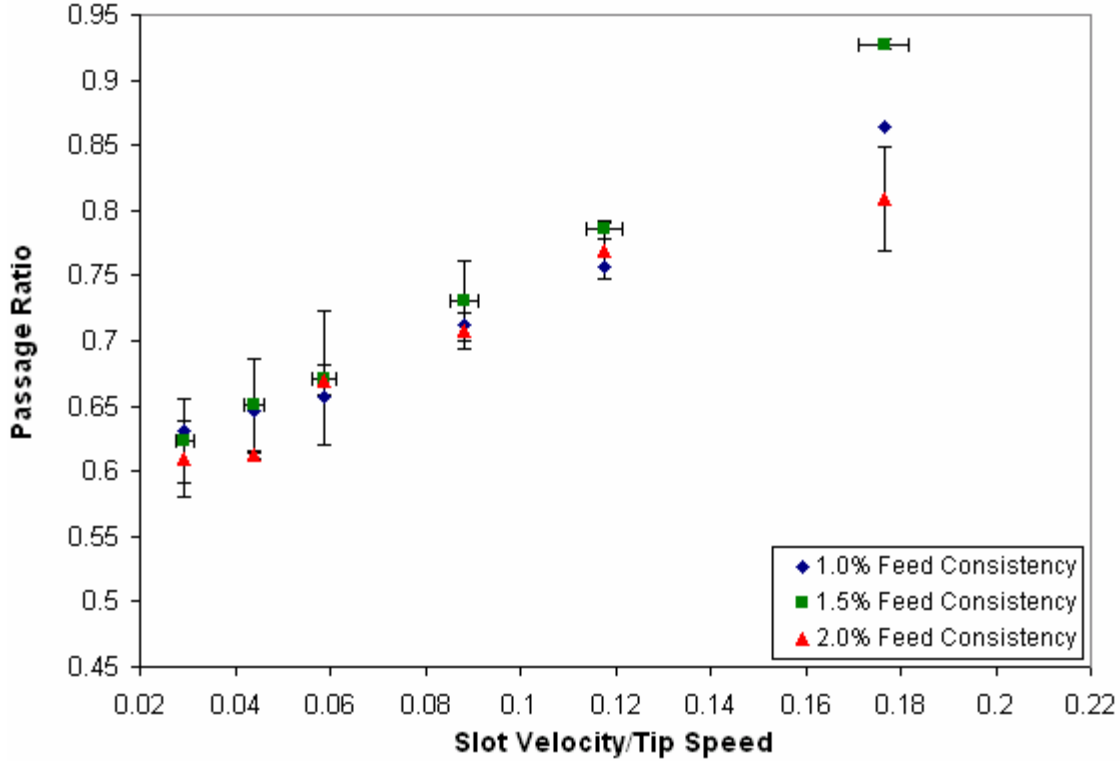


FIGURE 4.1: Passage Ratio vs. Slot Velocity
0.6mm contour height

For the low contour height screen, 0.6mm (Figure 4.1), the passage ratio was found to be approximately the same for every consistency at low slot velocities. For higher slot velocities there is a separation that is started to appear. This is more apparent for slot velocity of 3m/s or slot velocity /tip speed of 0.18. The reason for this is that the increase in slot velocity assists in the passage of fibres through the slot. The lack of variation in accept passage could be attributed to the fact that contour does not produce enough kinetic energy to disturb the fibre flocs near the surface of the screen to allow unhindered movement and easy passage. The horizontal error bars represent a propagation error in slot velocity caused by variations in actual slot widths and flow rate (calculation shown in Appendix G). The vertical error bars represent a standard deviation.

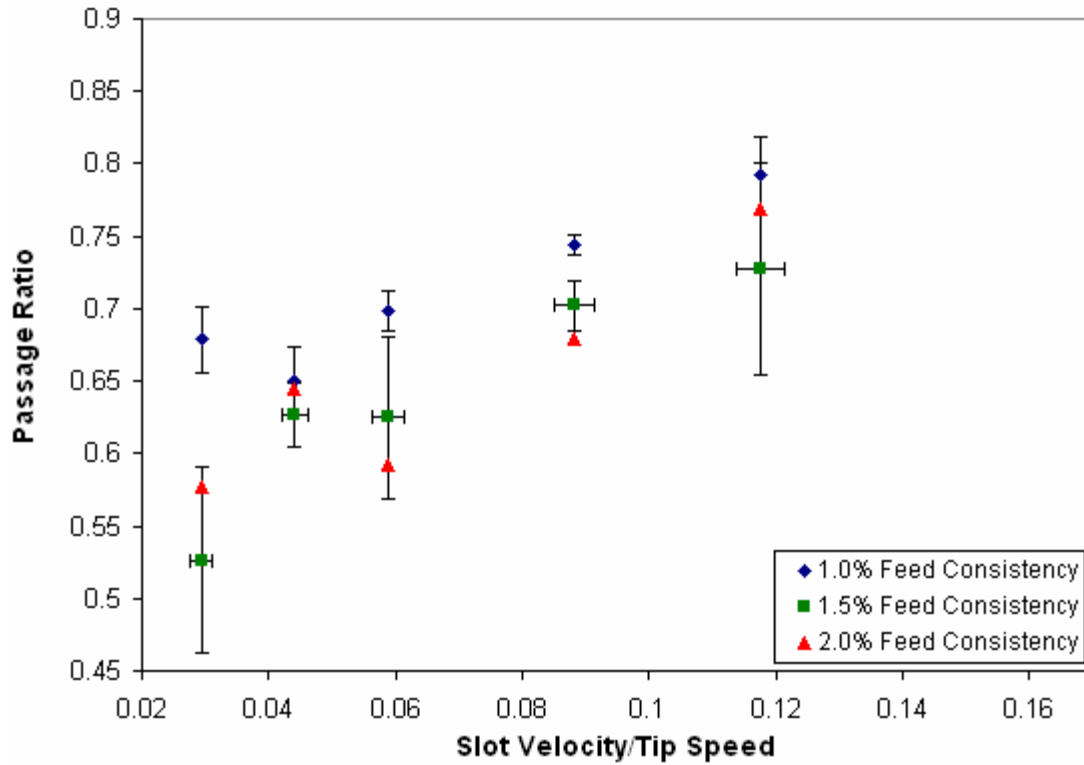


FIGURE 4.2: Passage Ratio vs. Slot Velocity
0.9mm contour height

The variation in the magnitude of the passage ratio for the different feed consistencies is larger for the 0.9mm contour height, 0.03 (Figure 4.2), than the 0.6mm contour height, 0.1 (Figure 4.1). The passage ratio for the 1.0% feed consistency increased while the 1.5% and 2.0% feed consistency appeared to remain the same. The increase in contour leads to a larger dispersion of kinetic energy to the fibre flocs, leading to un-hindered passage of fibres.

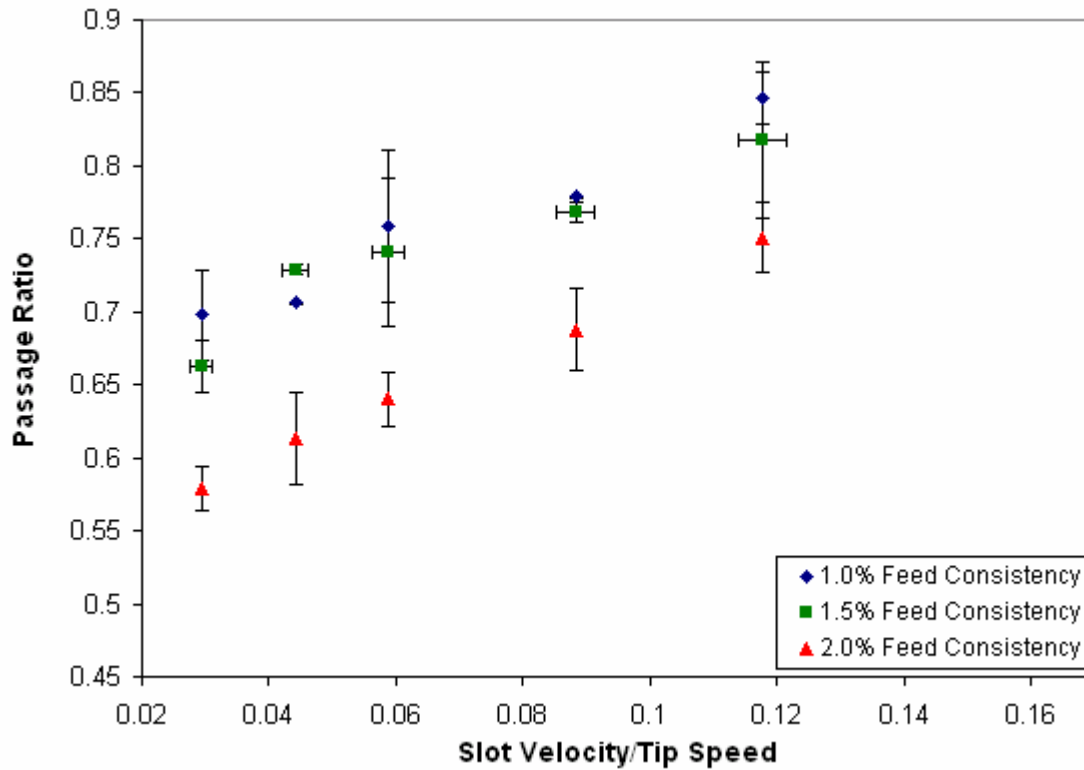


FIGURE 4.3: Passage Ratio vs. Slot Velocity
1.2mm contour height

With the increase in the contour height there is a larger separation between the low and the higher consistency feed. For 1.0% and the 1.5% feed consistency the magnitude of passage ratio is greater than that of the 2.0%, by a value of 0.13 (Figure 4.3). Looking at the 2.0% feed consistency for all their contour heights (Figures 4.1, 4.2, 4.3) there is no variance in the magnitude of passage ratio. The capacity of the screens was also found to decrease with the increase in contour height (Figures 4.4, 4.5, 4.7). The bars on the graph represent a 95% confidence conducted 4 tests for the 2.0% feed consistency on the 1.2mm contour height.

4.2 Effect of Feed Consistency on Passage Ratio

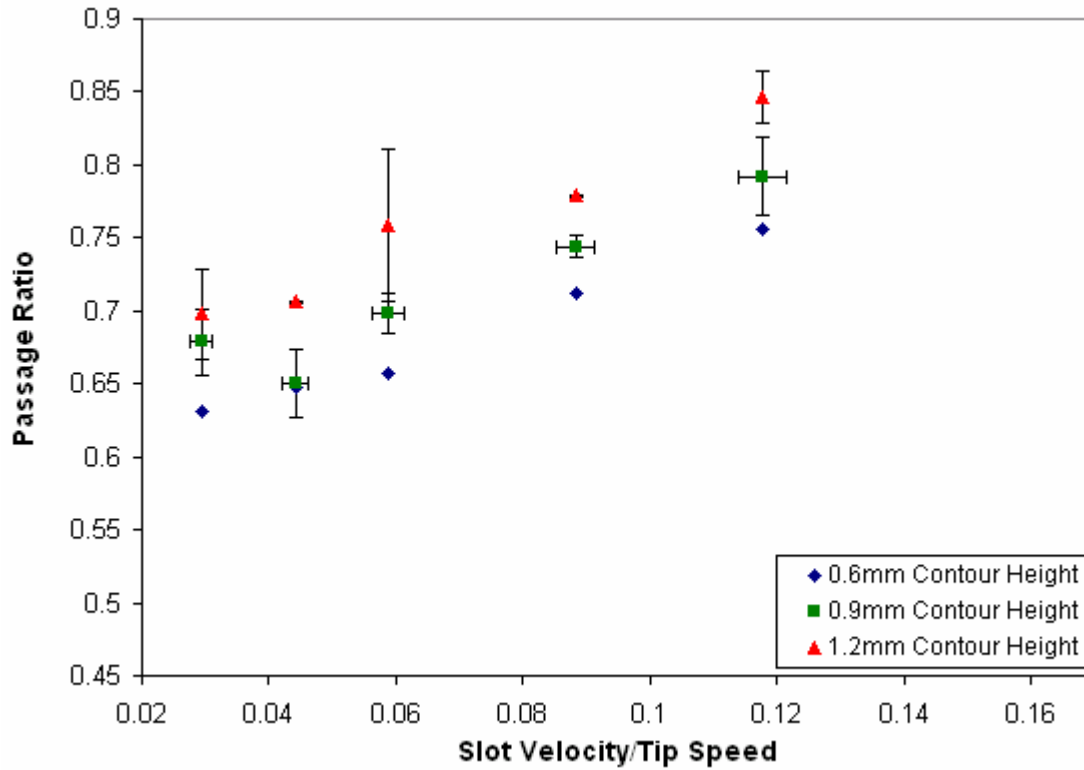


FIGURE 4.4: Passage Ratio vs. Slot Velocity
1.0% feed consistency

A higher passage with increasing contour height is expected when looking at the Passage Ratio vs. Slot Velocity/Tip Speed graph for different contour heights at constant feed consistency. In Figure 4.4, for the 1.0% feed consistency the results follow what is theoretically expected. The 1.2mm contour height was found to have the highest passage ratio while the 0.6mm had the lowest value. This shows that, at 1.0% feed consistency, the energy dispersed to the fluid has a large effect in assisting the passage of fibre through the screen.

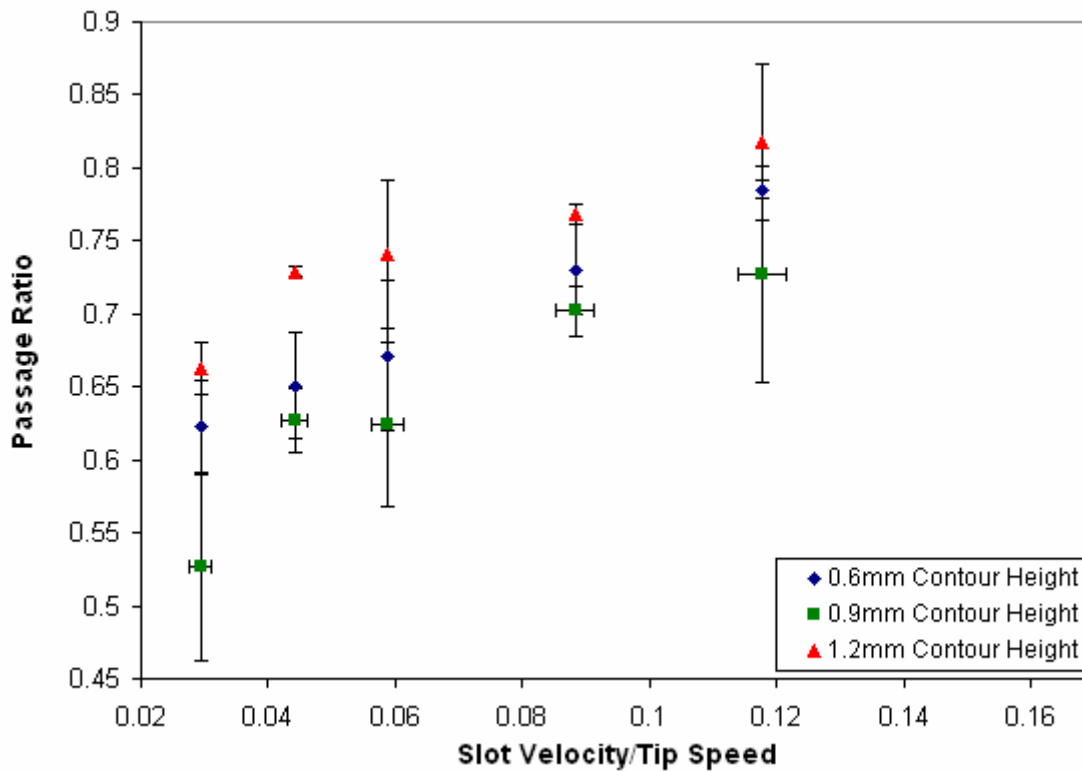


FIGURE 4.5: Passage Ratio vs. Slot Velocity
1.5% feed consistency

In Figure 4.5, for the 1.5% feed consistency, the results do not follow what is theoretically expected. The 1.2mm contour height was again found to have the highest passage ratio while the 0.9mm was now greater than the 0.6mm. The test for 1.5% feed consistencies were conducted in duplicate and the results attained were nearly identical. This observation is consistent with previous experimental data obtained by Saurabh Kumar [16], a former PhD student, using the same equipment. He found the same deviation. The 0.9mm contour height had the highest passage while the 1.2mm had the lowest. Kumar's results do not match the results shown in Figure 4.5 is because his experiments used a different type of pulp furnish as well as a different volumetric reject ratio and feed consistency. The test he conducted was at a feed consistency of 1.0% and the pulp was a 50/50 mixture of Kraft softwood/hardwood and a volumetric reject of 0.1. This demonstrates that there is another mechanism that causes these deviations from the conceptual thought behind screening that as contour height increases passage increases.

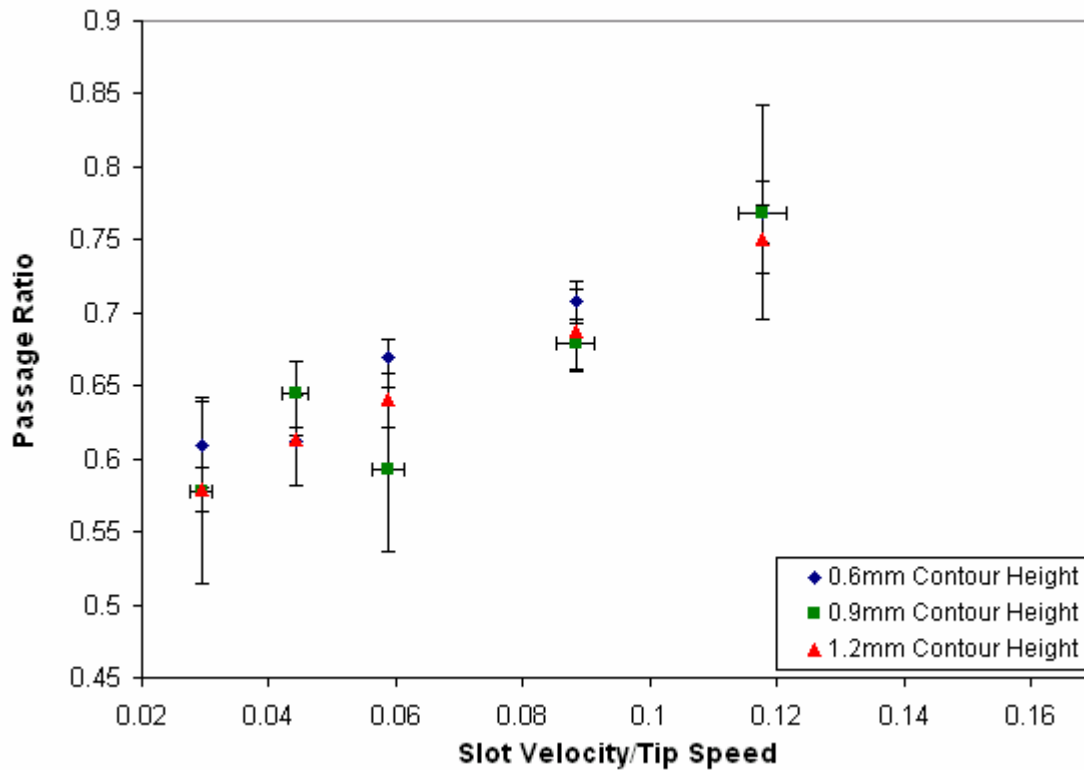


FIGURE 4.6: Passage Ratio vs. Slot Velocity
2.0% feed consistency

For the 2.0% feed consistency there was no significant difference in the fibre passage ratio between the different contour heights (Figure 4.7). For the 1.2mm contour height, the experiment was carried out 4 times to determine the reproducibility of the machine. From the data, confidence intervals were determined. Results were found to lay within a 95% confidence; as such, there is no statistical differences between the screen contour height at this feed concentration. This demonstrates that operation problems start to occur when screening at 2.0% consistency, fibre at the wall surface is not being dispersed. This could be caused by the fact that a foil rotor is being used, whereas a solid core rotor is more commonly used to screen high consistency feed [13]. The lack of variation could also be caused by contours do not disperse enough kinetic energy to fibres to break up flocs and allow for easier passage.

4.3 Effect of Contour Height on Accept Freeness.

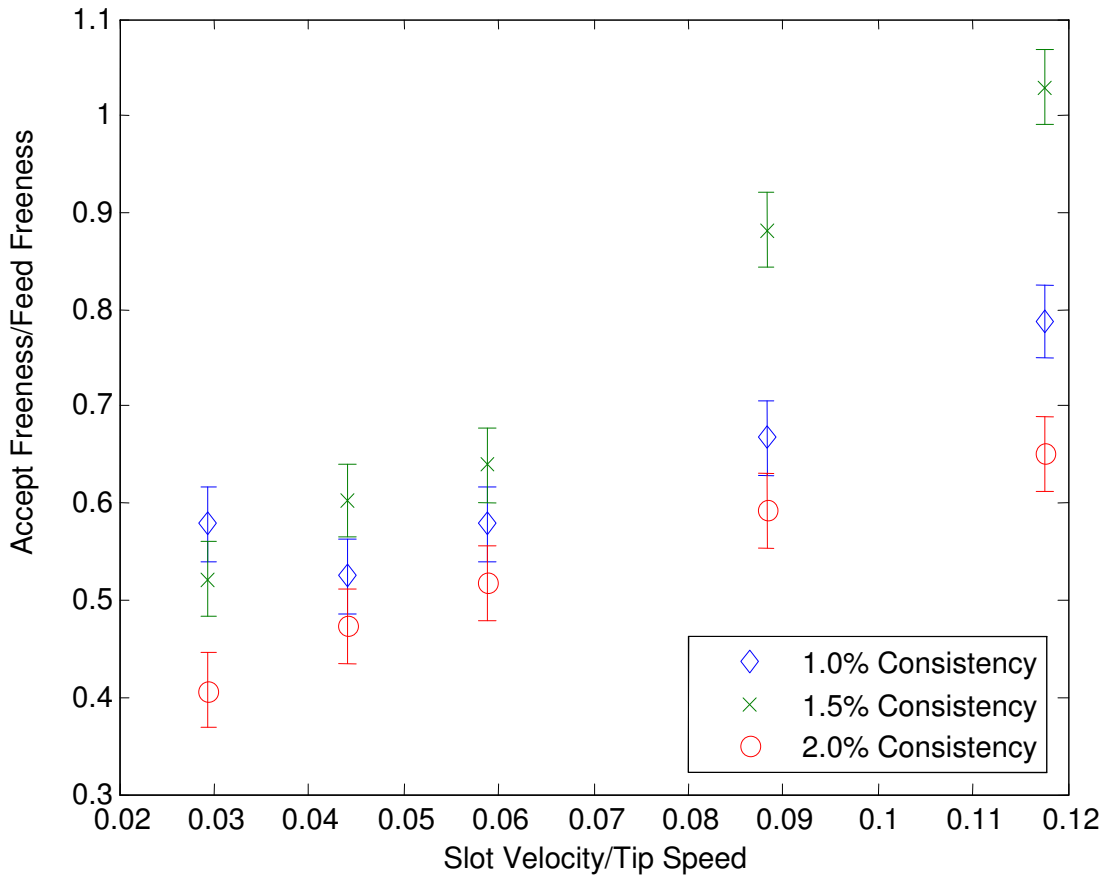


FIGURE 4.7: Accept Freeness vs. Slot Velocity
0.6mm contour height

The results for freeness closely follow the results of the passage ratio, Figure 4.1 and Figure 4.8. Figure 4.8 shows that there were minor variations in freeness due to consistency. The slot velocity has a greater effect on the freeness. This is attributed to the higher velocities pushing through longer fibre lengths. The error bars correspond to a standard variance of +/- 5 milliliters in the test.

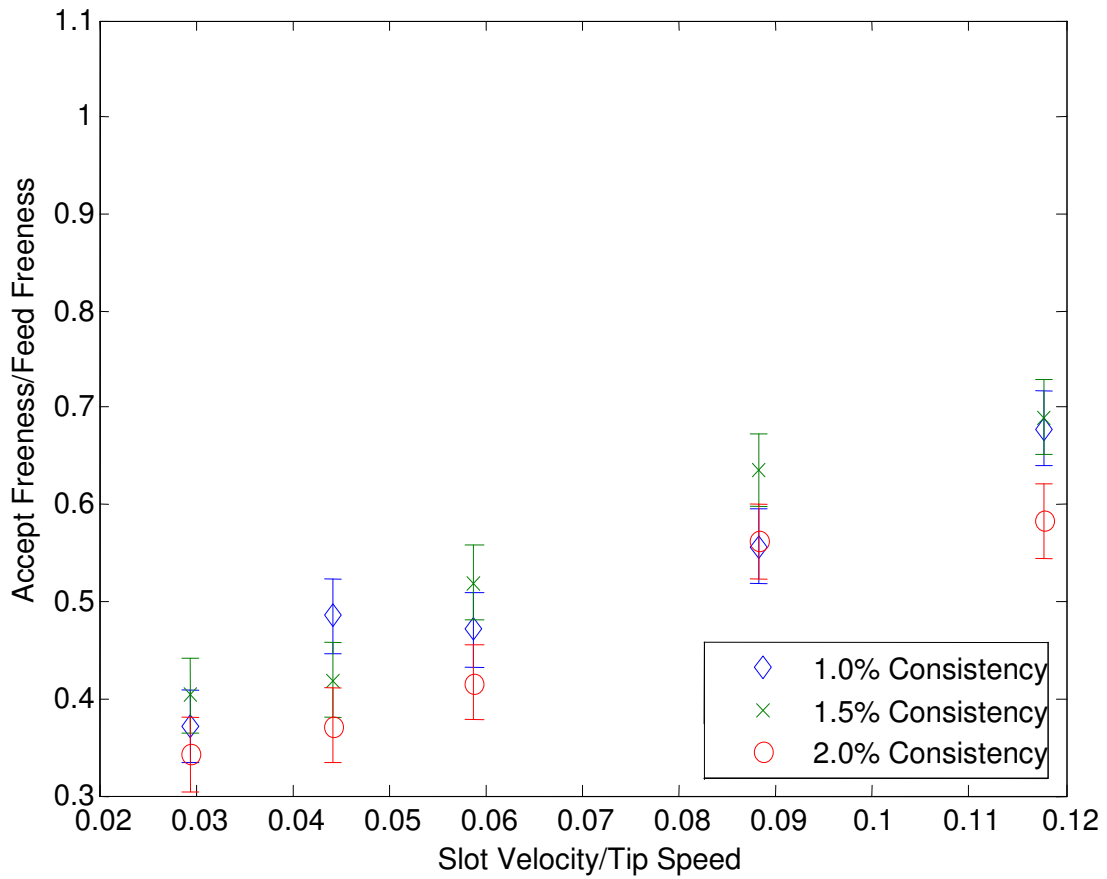


FIGURE 4.8: Accept Freeness vs. Slot Velocity
0.9mm contour height

For the 0.9mm contour height (Figure 4.9), the freeness is much lower than the 0.6mm screen at slot velocities/ tip speed of 0.3 and 0.6. This would mean that this screen is allowing more short fibres to pass than 0.6mm contour height. Again there is no major variation in freeness with respect to consistency and slot velocity seems to be a stronger variable.

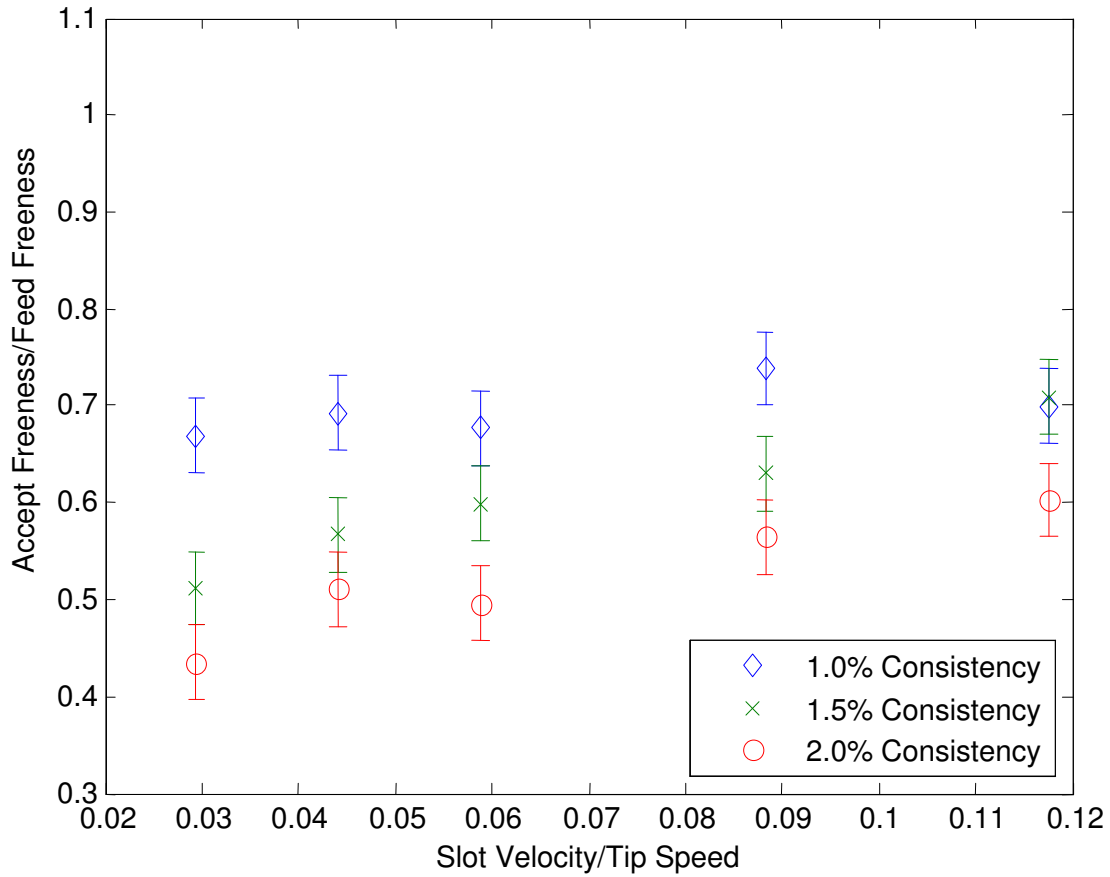


FIGURE 4.9: Accept Freeness vs. Slot Velocity
1.2mm contour height

The 1.2mm contour (Figure 4.10) shows the largest variation in freeness due to changes in feed consistency. The change in freeness due to changes in slot velocity is very minor and much lower compared to the 0.6mm and the 0.9mm contours. The increase in contour leads to easier passage for fibre so higher slot velocities are not needed to attain higher freeness as shown by the 1.0% feed consistency data (Figure 4.10). The 1.5% and 2.0% consistency data show minor dips at the lower slot velocity but flatten out at the higher slot velocities. This shows that the energy put into the fibre at the surface of the screen at slower slot velocities is larger at 1.0% consistency, then at 1.5% and 2.0%.

4.4 Effect of Feed consistency on Accept Freeness.

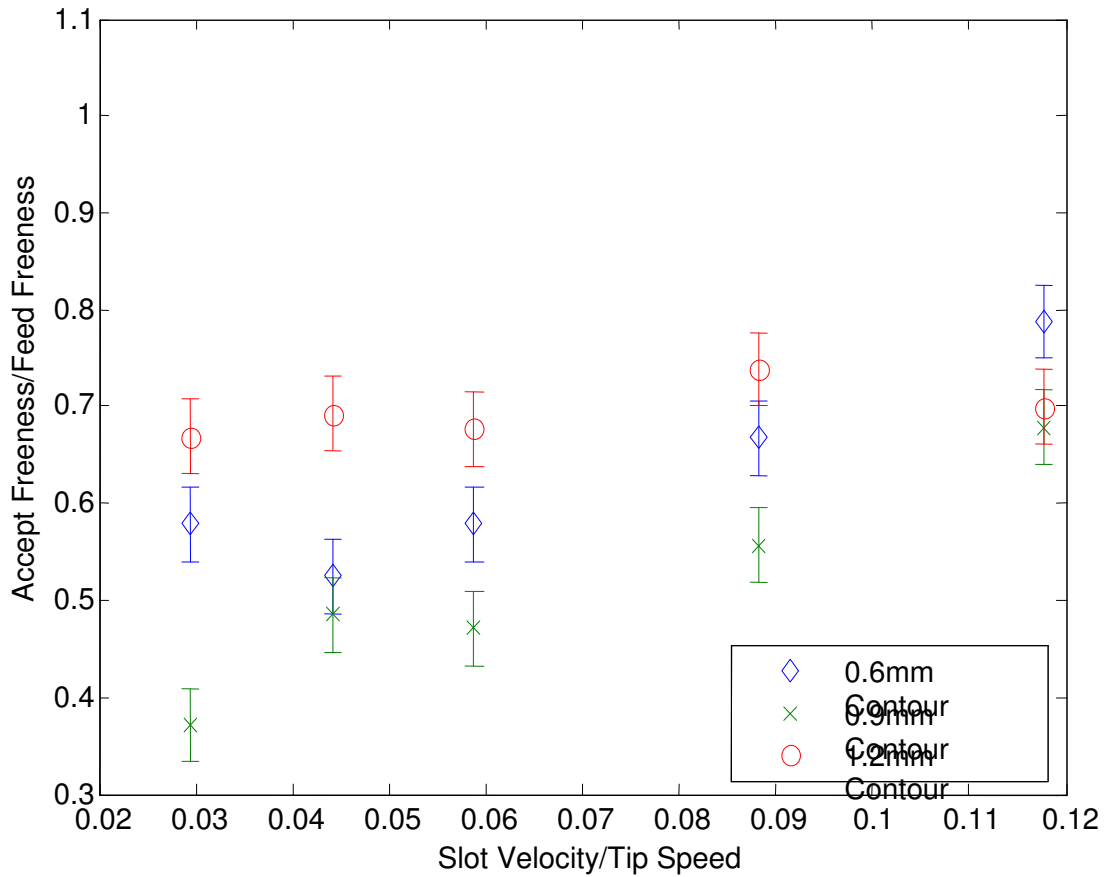


FIGURE 4.10: Accept Freeness vs. Slot Velocity
1.0% feed consistency

Figure 4.11 shows that 1.2mm contour height has the largest freeness. However, the 0.6mm has higher passage ratio compared to the 0.9mm contour. This follows the trend of Accept Fibre length vs. Slot velocity (Appendix B.4): the 0.6mm contour height has a larger length than the 0.9mm contour height.

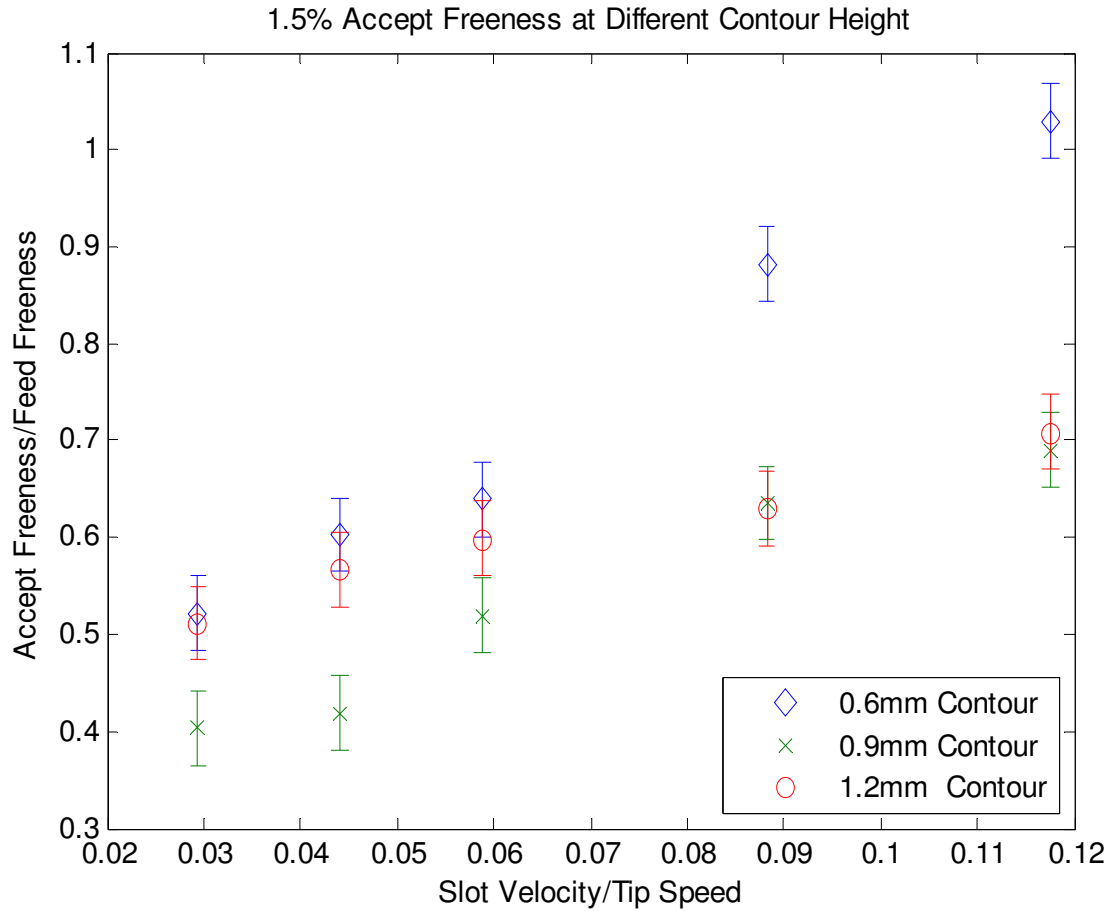


FIGURE 4.11: Accept Freeness vs. Slot Velocity
1.5% feed consistency

The accept freeness, at 1.5% feed consistency, is found to decrease at the lower slot velocities (Figure 4.12), for the 1.2mm and 0.6mm. Compared to Figure 4.11, the magnitude of the accept freeness has dropped by 0.12-0.2. The increase in feed concentration leads to larger flocs which act as a natural barrier (screen), which only allows the smaller fibres to approach the slot. Figure 4.13 shows this behavior greater for the 2.0% feed consistency

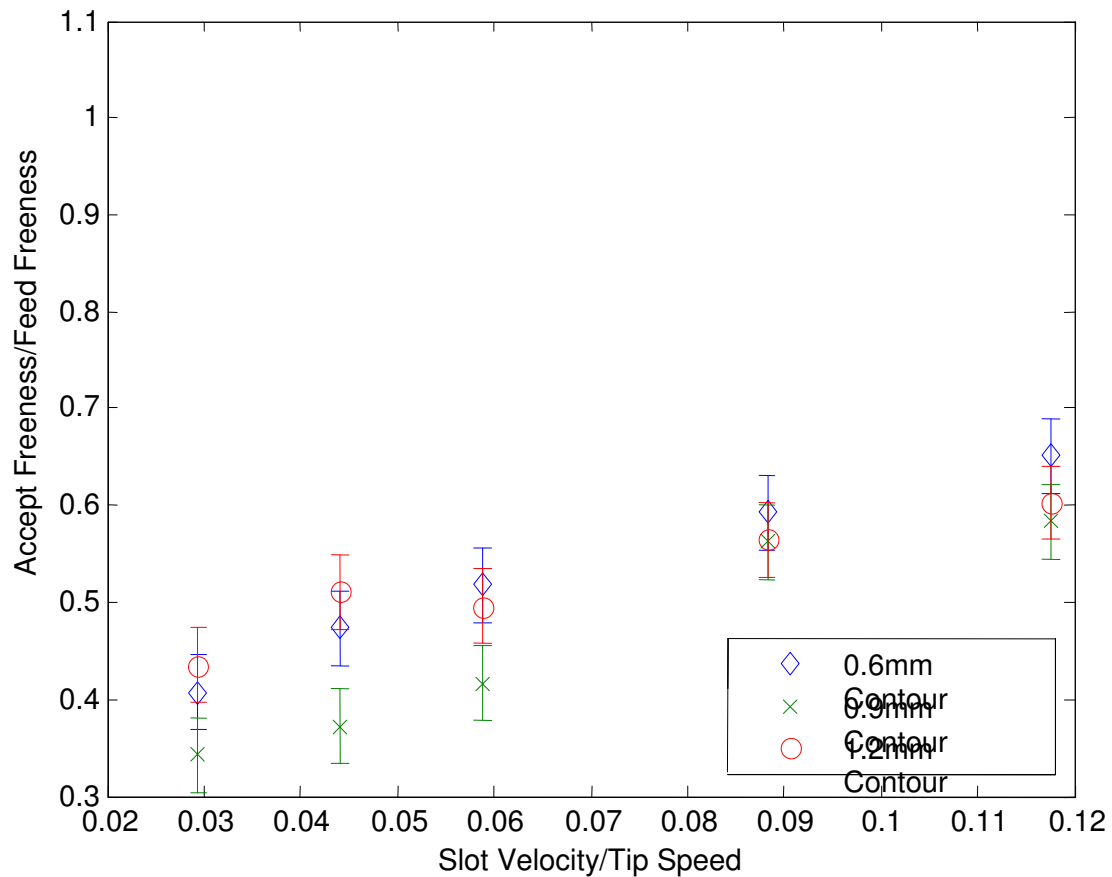


FIGURE 4.12: Accept Freeness vs. Slot Velocity
2.0% feed consistency

For the 2.0% feed consistency there is a trend that is similar to that found for the 1.0% consistency. The 1.2mm had a higher freeness at the low slot velocities; however, at the higher slot velocities all the contour heights had the same level of freeness. Again the 0.6mm had greater freeness than the 0.9mm. However within a 5mls variance there is no significant difference in the freeness. This corresponds to the results of fibre length, shown in Figure B.6, which has no significant difference between the screens.

4.5 General Discussion

In addition to the results shown above, fibre length and fibre coarseness data were attained. Fibre length data is shown in Appendix B and coarseness data is shown in Appendix C. There was very little variation in fibre length due to contour height and feed consistency. The slot velocity had the largest affect on the fibre length (Figure B.4-B.6). The coarseness was found not to vary significantly with feed consistency for all contour height (Figure C.1-C.3). However, there were some changes due to slot velocity, for the 1.2mm contour height, Figure C.6. The magnitude change is not significant, and any difference can fall within experimental variance. To determine how accurate the experimental test was on accept fibre length and accept coarseness, a 95% confidence was used to determine the variance (Figure B.6 and Figure C.6). To test the accuracy of the FQA, a sample was run through the machine 11 times and from that data a confidence interval of 95% was calculated. It was found that the FQA accurately calculated the coarseness; this is shown in Figure B.1. The bars represent a 95% confidence from a sample of 11 tests.

From investigating the factors affecting screening, the largest influence was found to be the slot velocity. The slot velocity helps the fibre near the surface of the screen align perpendicular to the surface of the screen to allow for passage.

The second major factor was the contour height. The contour height has the ability to introduce kinetic energy into the fibres close to the screen surface; this allows for fibre flocs to break up into individual strands. Having the flocs broken up at the screen surface is desirable because it allows the strands to orientate themselves properly, without hindrance, to pass into the screen aperture. Consequently, higher contour height leads to larger passage ratios.

The third most important factor is the feed consistency. When feed consistency is increased then larger, more tightly-bound flocs are formed at the screen surface. These flocs would require tremendous amount of energy to break them apart; this energy comes

from the rotor element and the screen surface. If these flocs are not broken up they will prevent the free fibres from approaching and orientating themselves to pass through the screen aperture. This was shown in Figure 4.3. For low consistencies the 1.2mm contour breaks the flocs allowing for higher passage ratios; however, the high consistencies still have a low passage ratio.

CHAPTER 5: NUMERICAL ANALYSIS

The second objective of this research was to develop an expression for freeness drop on the accept side of the screen as a function of the studied variables. The first step was to come up with a relation for passage ratio with respect to screening factors. The factors studied were contour height, slot velocity, and feed consistency.

5.1 Dimensional Analysis.

Buckingham Pi theory was applied to determine non-dimensional parameters. The variables that control screening were determined to be fibre passage (P), feed concentration (C), slot velocity (V_s), tip speed (V_t), rotor gap (g), contour height (H), wire width (W_s), wire slot (W_w), volumetric reject (R_v), viscosity (μ) and density (ρ).

$$\phi(P, C, V_s, V_t, g, H, W_s, W_w, R_v, \mu, \rho) = 0$$

Variables = 10

Units = 3

Dimensionless number = 10-3 = 7

The three fundamental physical quantities are mass (m), length (l) and time (t).

The variables chosen: V_t , ρ , g.

The Pi groups were:

$$\begin{aligned}\Pi_1 &= V_t^{a1} g^{b1} \rho^{c1} C \\ \Pi_2 &= V_t^{a2} g^{b2} \rho^{c2} V_s \\ \Pi_3 &= V_t^{a3} g^{b3} \rho^{c3} H \\ \Pi_4 &= V_t^{a4} g^{b4} \rho^{c4} \mu \\ \Pi_5 &= V_t^{a5} g^{b5} \rho^{c5} R_v \\ \Pi_6 &= V_t^{a6} g^{b6} \rho^{c6} W_s \\ \Pi_7 &= V_t^{a7} g^{b7} \rho^{c7} W_w \\ \Pi_8 &= V_t^{a8} g^{b8} \rho^{c8} P\end{aligned}$$

Solving these groups' results in:

$$\begin{aligned}\Pi_1 &= \frac{C}{\rho} & \Pi_5 &= R_v \\ \Pi_2 &= \frac{V_s}{V_T} & \Pi_6 &= \frac{W_s}{g} \\ \Pi_3 &= \frac{H}{g} & \Pi_7 &= \frac{W_w}{g} \\ \Pi_4 &= \frac{\mu}{gV_T\rho} = Re^{-1} & \Pi_8 &= P\end{aligned}$$

So passage of fibre was found to be a function of these four Pi variables:

$$P = \phi(\Pi_1, \Pi_2, \Pi_3, \Pi_4, \Pi_5, \Pi_6, \Pi_7) \quad (eqn : 5.1)$$

5.2 Equation for Passage Ratio.

The first equation tested was a power law relation (Equation 5.2). The Microsoft Excel worksheet is provided in Appendix E.1.

$$P = a(Re)^{-b}(R_v)^c \left(\frac{C}{\rho}\right)^d \left(\frac{V_s}{V_T}\right)^e \left(\frac{H}{g}\right)^f \left(\frac{W_s}{g}\right)^g \left(\frac{W_w}{g}\right)^h \quad (eqn : 5.2)$$

Using the Solver program in Excel, the values of the constants were found and are shown below.

a	b	c	d	e	f	g	h
1.106	-0.04785	0.009833	0.069059	0.17761	0.052908	-0.1292	0.010863

Table 5.1: Results for Fitting Parameters equation.5.2

This result seems to predict the passage relatively accurately ($R^2 = 0.782$); however, an alternative equation was also tested to determine a better fit. The second equation tested had the form:

$$P = \left(\frac{V_s}{V_t} \right)^B \quad (\text{eqn : 5.3})$$

The Excel worksheet for Equation 5.3 is in Appendix E.2. This equation was chosen since, from the graphs in chapter 4 (Figure 4.1-4.3), the largest influence on passage was the slot velocity. The constant B was found to be a function of both the feed consistency and the contour height. The results are shown in Table 5.2.

Consistency WT%	CONTOUR HEIGHT								
	0.6mm			0.9mm			1.2mm		
	B	CI	R ²	B	CI	R ²	B	CI	R ²
1	0.133	0.089	0.909	0.120	0.069	0.745	0.096	0.086	0.892
1.5	0.128	0.121	0.849	0.156	0.124	0.825	0.104	0.089	0.841
2	0.141	0.055	0.926	0.154	0.109	0.764	0.153	0.055	0.918

Table 5.2: Result for fitting parameters for equation 5.3 and R^2

The black values represent the constant B , the green represent a 95% confidence interval and the red values represent the R^2 value (comparing the experimental values with the calculated values). The graph below shows how B varies with contour height and concentration, which is represented by C/ρ . The horizontal marks represent the upper and lower limits of a 95% confidence interval.

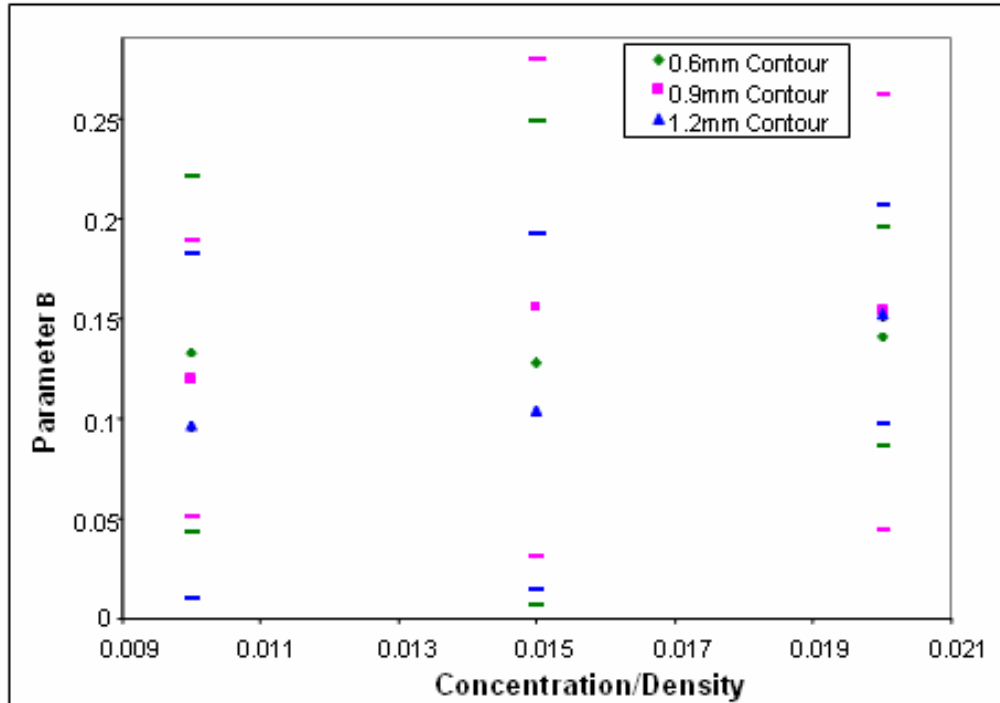


Figure 5.1: Fitting parameter B variation with concentration and contour height.

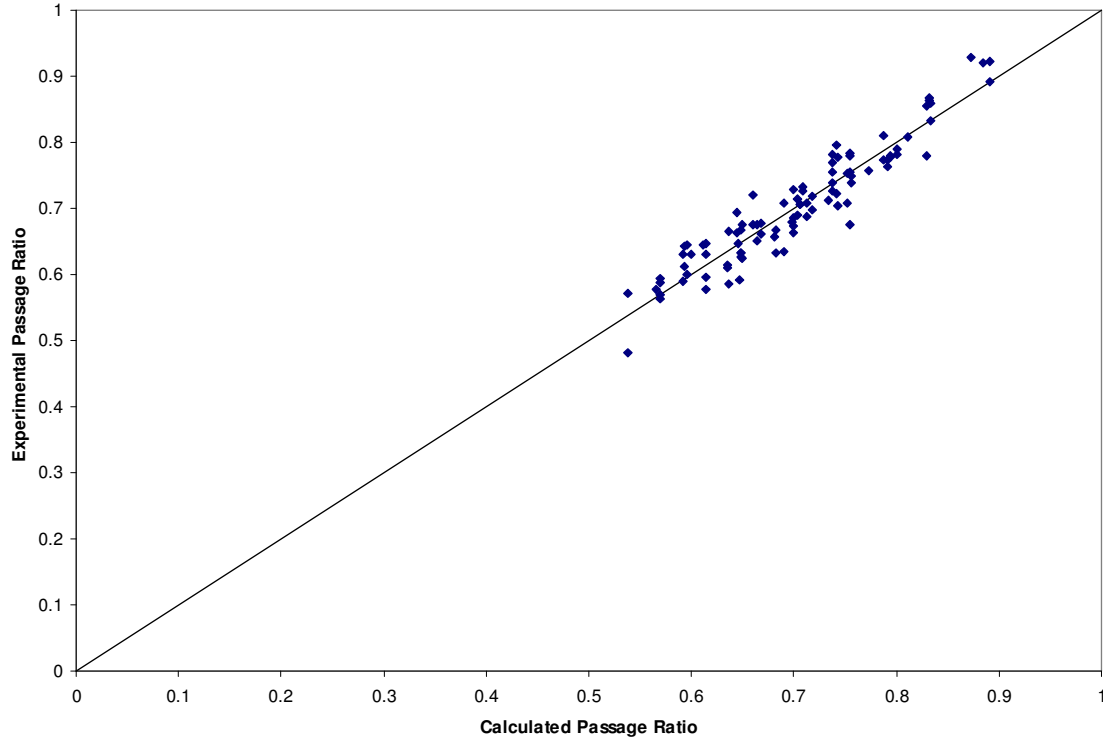


Fig 5.2: Experimental Passage vs. Calculated Passage Ratio

Figure 5.2 shows that there is not a lot of scatter in the data. As seen in Table 5.2, equation 5.3 fits the data better. B is a strong function of the consistency and the contour height (Figure 5.1). We again see the inversing effect for the 1.5% feed consistency on the 0.9mm contour height. As stated before, this run was reproduced and the results obtained were similar to the results of the first run. There seems to be a consistency at which an inflection in the function of B occurs. This could be representative for every screen cylinder. However, in the tests conducted the inflection was not reached for 0.6mm and the 1.2mm contour heights. However, Figure 5.2 does not have enough consistency points to provide a good estimate of the value of B . To get a better result for this parameter, the screens should be run at consistencies $<1\%$ and run two to three other

feed consistencies between 1% and 2%. At consistencies > 2%, the operational limits of the screen would be approached.

5.3 Equation for Accept Freeness.

The next step was to determine a relationship between freeness and passage ratio. Figure 5.3 shows a plot of Accept Freeness vs. Passage Ratio. The worksheet showing the derivation of the freeness equation is shown in Appendix E.3.

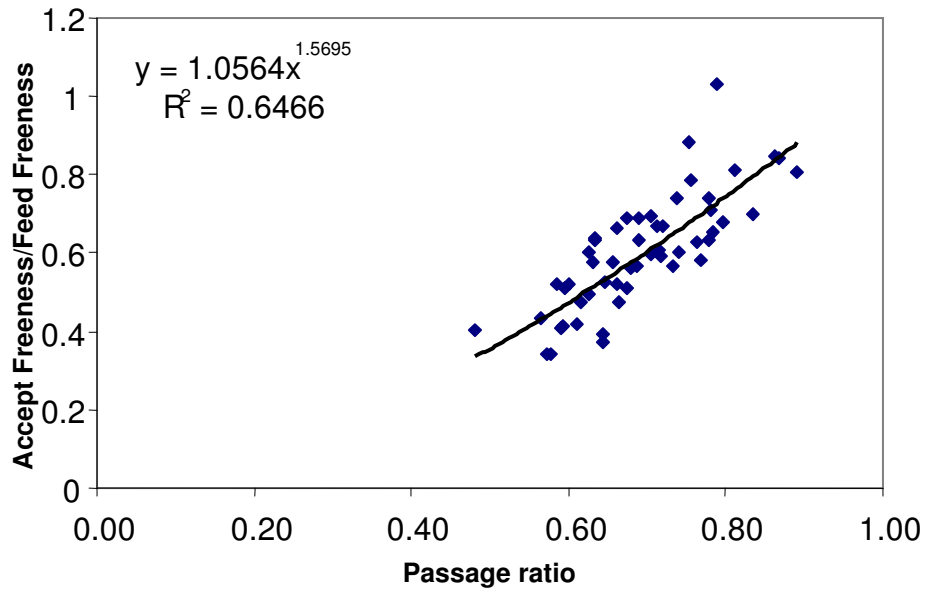


Figure 5.3: Plot of Freeness vs. Passage ratio.

Using the equation shown in Figure 5.3 and the equation derived for passage ratio (Equation 5.3), equation 5.4 was derived:

$$F = 1.0564 \left(\frac{V_s}{V_t} \right)^{1.5696B} \quad (eqn : 5.4)$$

The following results were obtained from testing Equation 5.4 with the experimental data:

C (wt %)	R ²		
	0.6mm	0.9mm	1.2mm
1.00%	0.87	0.82	0.7
1.50%	0.95	0.95	0.96
2.00%	0.99	0.94	0.93

Table 5.3: R² for fitting parameters in Table5.2 using equation 5.4

From using equation 5.4 and applying the constants in Table 5.2, the model was found to be a good representation of the experimental data. Figure 5.4 shows that there is not a lot of scatter.

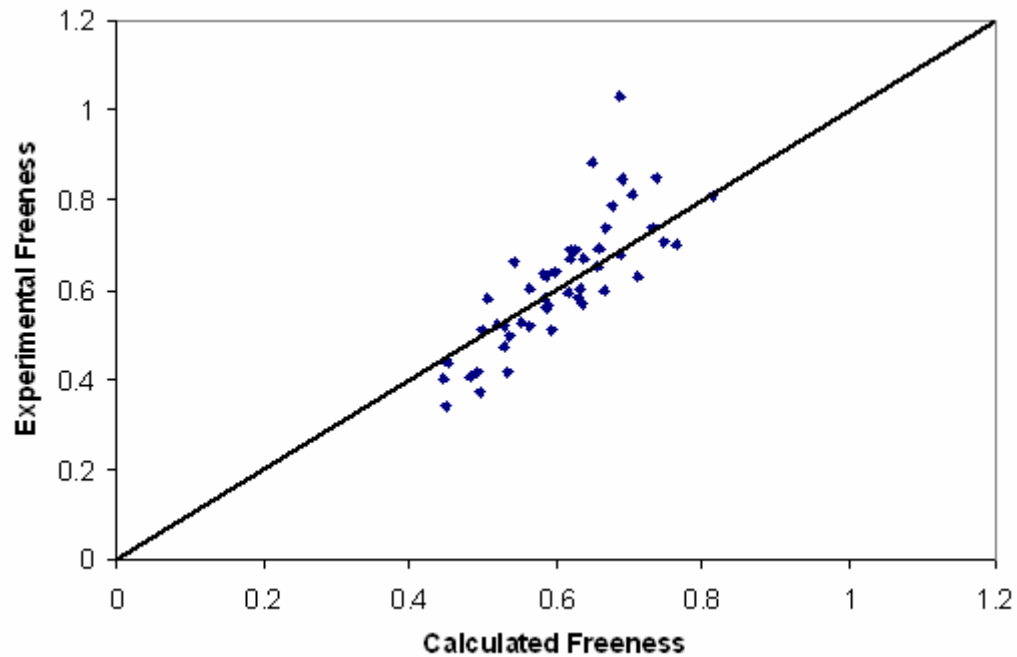


Figure 5.4: Experimental Freeness vs. Calculated Freeness.

CHAPTER 6: CONCLUSION

The overall objectives of this study were attained; however, new questions also were raised. First objective was to determine which operating parameters had the greatest influence (contour height, slot velocity, feed consistency) and second was to develop a freeness model for screen accepts.

Of the three main variables studied, the slot velocity had the greatest influence on the passage ratio and freeness. As the slot velocity increased a greater force was applied to the fibre to help push it through the screen aperture. However, this increase in slot velocity decreases the fractionation ability of the screen. The increased force would have enough energy to pull a fibre through that would most likely have been rejected at low slot velocities.

The second most important variable was the contour height. The main function of the contour height is to disrupt the flow of thick stock at the wall of the screen and allow for unhindered movement of fibre to the screen wall. The 0.6mm contour screen was found to produce inadequate amounts of energy to disrupt the flow near the wall; this was seen with the low passage ratios and with the limited variation between the different feed consistencies. The larger contour heights were shown to have more variation in their passage ratios. Comparing the passage ratio 1-2% feed consistencies for the 1.2mm contour, a very large separation between the 2% consistency and the other consistencies was found.

The third most important factor was the feed consistency. At low feed consistencies there is less crowding in the screen. Less crowding leads to more loosely-formed flocs, which are easier for the contour height and the rotor to dissipate and thus leads to unhindered movement. Thicker feed stock has a negative effect on passage. The 1.2mm contour height was not even strong enough to disrupt the flocs formed with a feed consistency of 2.0%. As the feed concentration increased, the freeness was found to decrease. This means that the large flocs act like a natural barrier, preventing the longer fibres from

passing into the accept side. Thus only smaller fibres are able to pass between flocs and get accepted.

In addition to these observations, a new freeness model was developed. This model describes the ratio between feed freeness and accepts freeness. The freeness was found to be proportional to the slot velocity/tip velocity to the power of fitting constant B . The fitting parameter B was found to be dependent on both the feed consistency and the contour height. The developed equation shows a good relationship between the experimental passage and the calculated passage.

APPENDIX A: REFERENCES

1. Ammälä A., Dahl O., Kuopanportti H., and Jouko Niinimäki J., "Pressure screening: changes in pulp properties in the screen basket" *Tappi Journal*, 99-105, October 1999.
2. Ammälä A., PhD thesis, "Fractionation of thermo-mechanical pulp in pressure screening, an experimental study on the classification of fibres with slotted screen plates". Dept. of process and Envi. Eng. Uni. of Oulu, Finland, 2001.
3. Atkins M., Walmsley M., Weeds Z., "Internal Fibre Length Concentration in a Pressure Screen", *Appita Journal*, 41-47, January 2007
4. Dong S., Salcudean M., and Gartshore I., "The Effect of Slot Shape on the Performance of a Pressure Screen", *Tappi Journal*, 3-7, May 2004, Vol. 3, No 5.
5. Gooding, R.W., "The passage of fibers through slots in pulp screening". M.A.Sc Thesis, University of British Columbia, 1986.
6. Gooding R.W., Kerekes, R.J., "The motion of fibres near a screen slot". *J. Pulp Paper Science*, 59-62, 15(1989):2.
7. Gooding R.W., Kerekes, R.J., "Derivation of Performance Equations for Solid-Solid Screens". *The Canadian Journal of Chemical Engineering* 67 801-805. (1989).
8. Jokinen H., "Screening and Cleaning of pulp- a study to the parameters affecting separation", PhD, Department of Process and environmental Engineering, University of Oulu, 2007
9. Jokinen H., Karjalainen M., Niinimäki J., & Ammala A., "Effect of Furnish Quality on Pressure Screen Performance", *Appita Journal*, 35-40, January 2007, vol. 60.
10. Jokinen H., Ammala A., Virtanen J.A., Lindroos K., & Niinimäki J., "Pressure Screen Capacity- Current Findings on the Role of Wire Width and Height", *Tappi Journal*, 3-10, Vol.6, No 1.
11. Jokinen H., Ammala A., Niinimäki J., Virtanen J.A., & Lindroos K., "Effect of Bar Geometry on Screen Plate Performance- A Laboratory Study on Pressure Screening", *Nordic Pulp and Paper Research Journal*, 451-459, Vol.21, no. 4/2006

12. Julien Saint Amand F & Perrin B., "Fundamentals of screening: Effect of rotor design and fibre properties". *Proc. TAPPI Pulping Conference*, Orlando, USA, 941-955. 1999
13. Krotscheck, A.W. (2006). Pulp Screening, Cleaning and Fractionation. In H.Sixta (Ed.) *Handbook of Pulp* (561-580), Wiley-VCH
14. Kumar, A., "Passage of fibres through screen apertures", PhD thesis, dept. Chem. Engg., Uni. British Columbia, 1992.
15. Kumar, A., Gooding R.W., Kerekes R. J., "Factors controlling the passage of fibres through slots" *TAPPI journal*, 247-254, May 1998.
16. Kumar, S., "Effect of Contour Height on Screen Performance - Fibre Fractionation and stickies removal", Masters thesis, dept. Chem. Eng., EFPG, 2004.
17. Mokamati S.V., Olson J.A., Gooding R.W., "The Effect of Wire Shape on the Flow Through Narrow Apertures in a Pulp Screen Cylinder" *2005 ASME Fluids Engineering Division Summer Meeting and Exhibition*, Houston, TX, USA, June 19-23, 2005.
18. Olson, J.A., "Natural Resources", Mech. Eng. Dept. University of British Columbia. www.mech.ubc.ca/~chbe401.
19. Olson, J.A., "Fibre length fractionation caused by pulp screening, slotted screen plates", *Journal Pulp Paper Science*. 27(8): 255-261, 2001.
20. Olson, J.A., "A Lecture in Pressure Screening". CHBE 401, University of British Columbia, February 2005.
21. Walmsley M., Weeds Z., "Feed Consistency and Rotor Effects on Pulp Screening Mechanisms and Reject Thickening", *Appita Journal*, 136-143, March 2007

APPENDIX B: ACCPET FIBRE LENGTH RESULTS

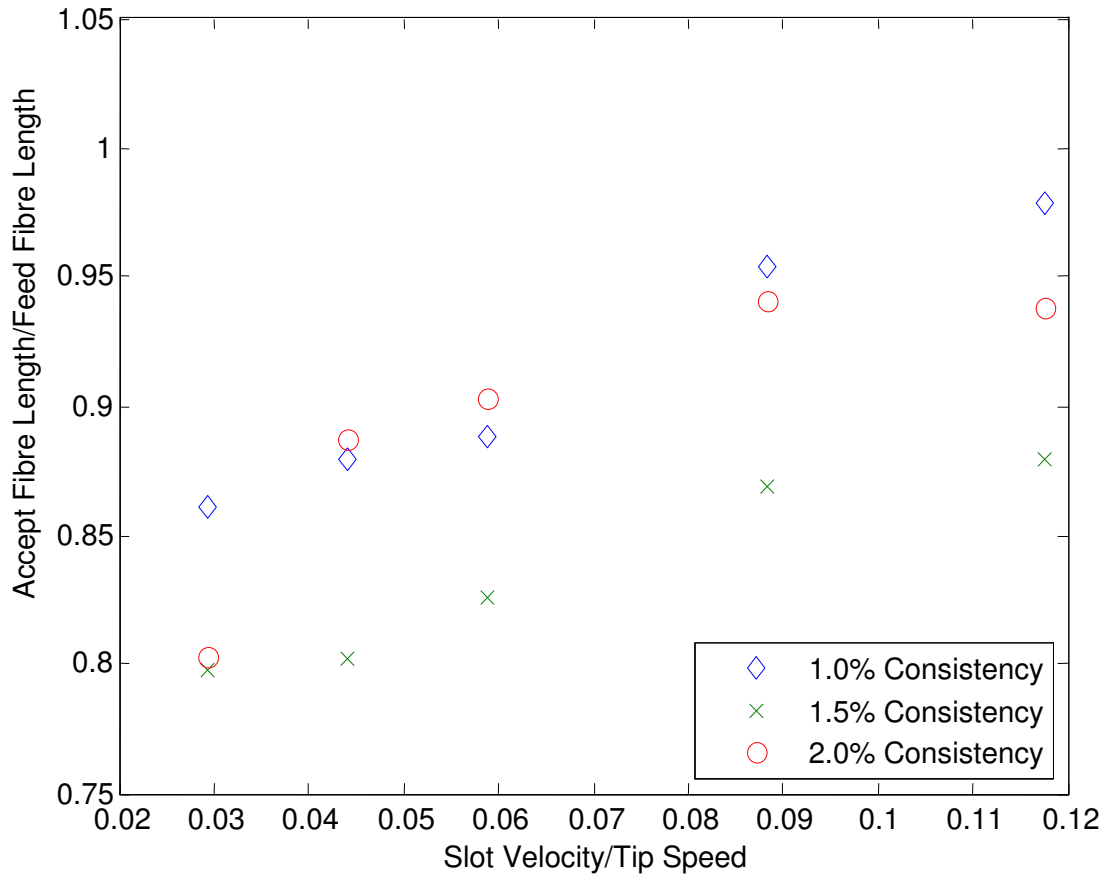


Figure B.1: Accept Fibre Length 0.6mm Contour Height

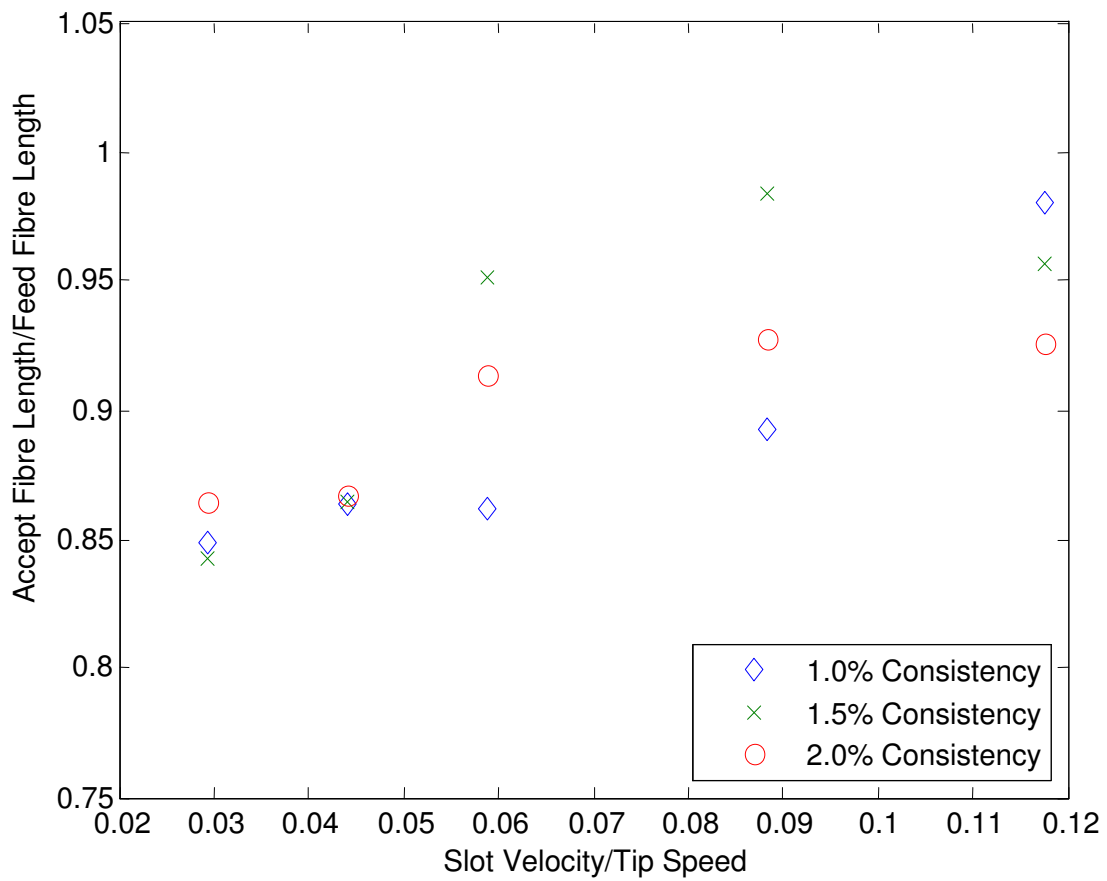


Figure B.2: Accept Fibre Length 0.6mm Contour Height

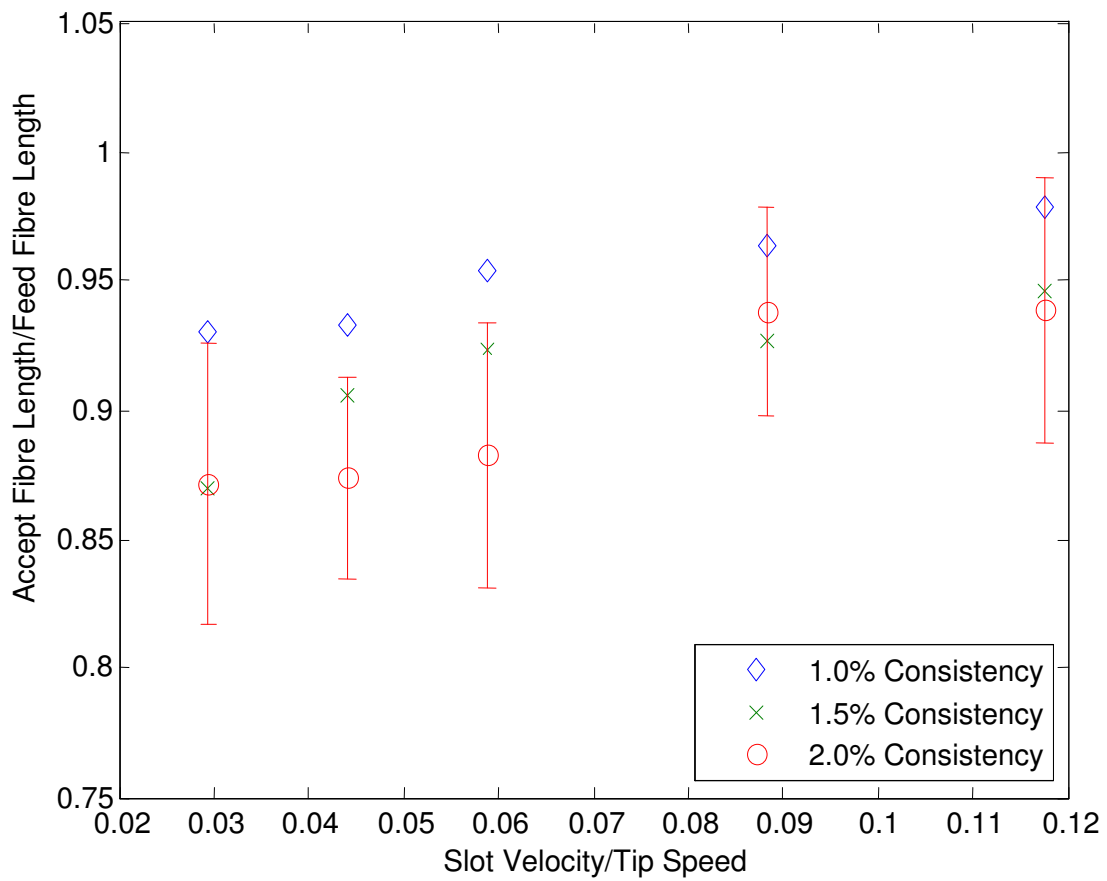


Figure B.3: Accept Fibre Length 1.2mm Contour Height

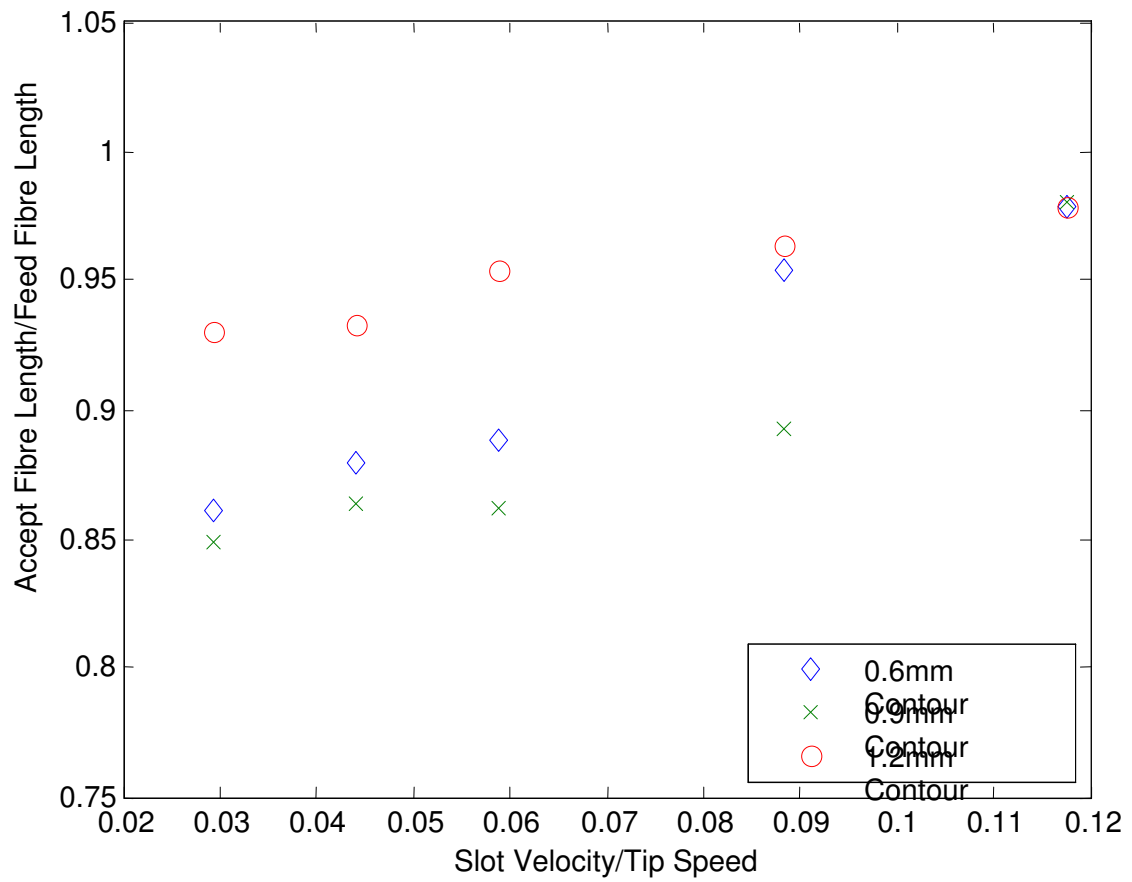


Figure B.4: Accept Fibre Length for 1.0% feed Consistency

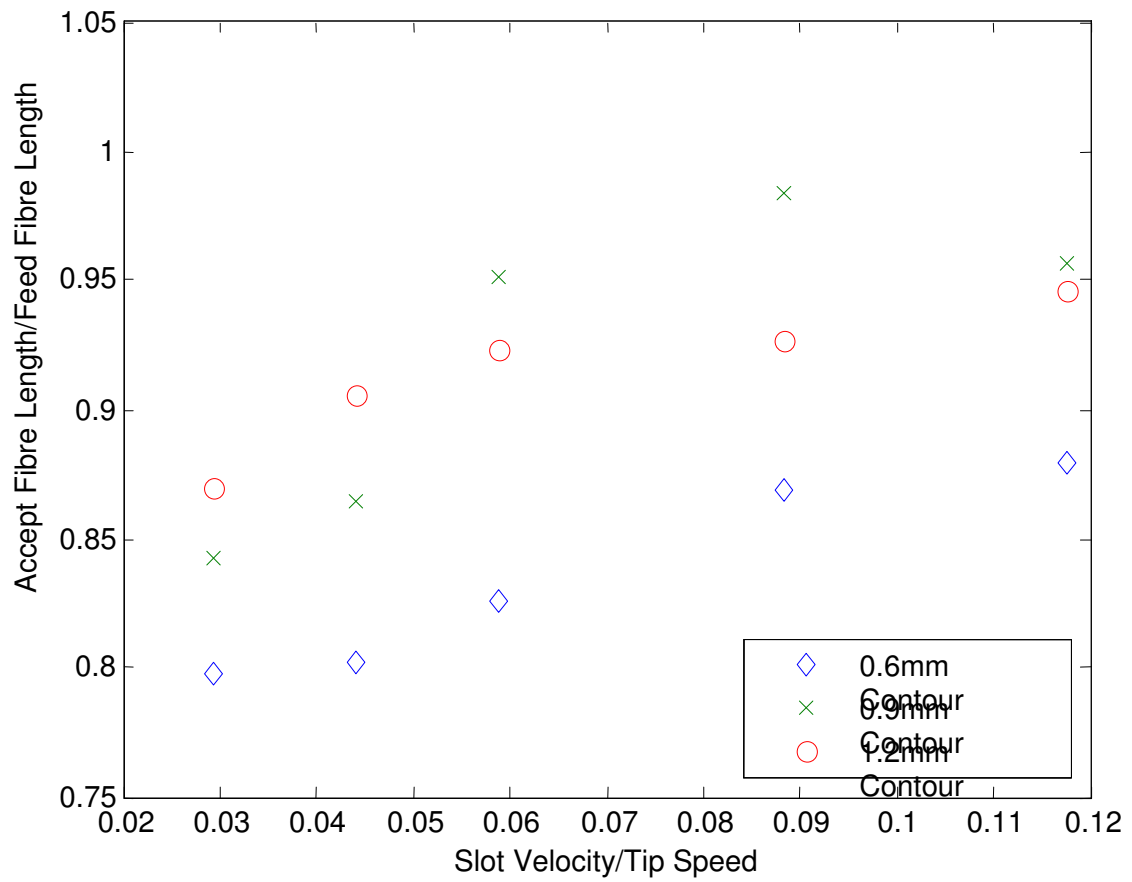
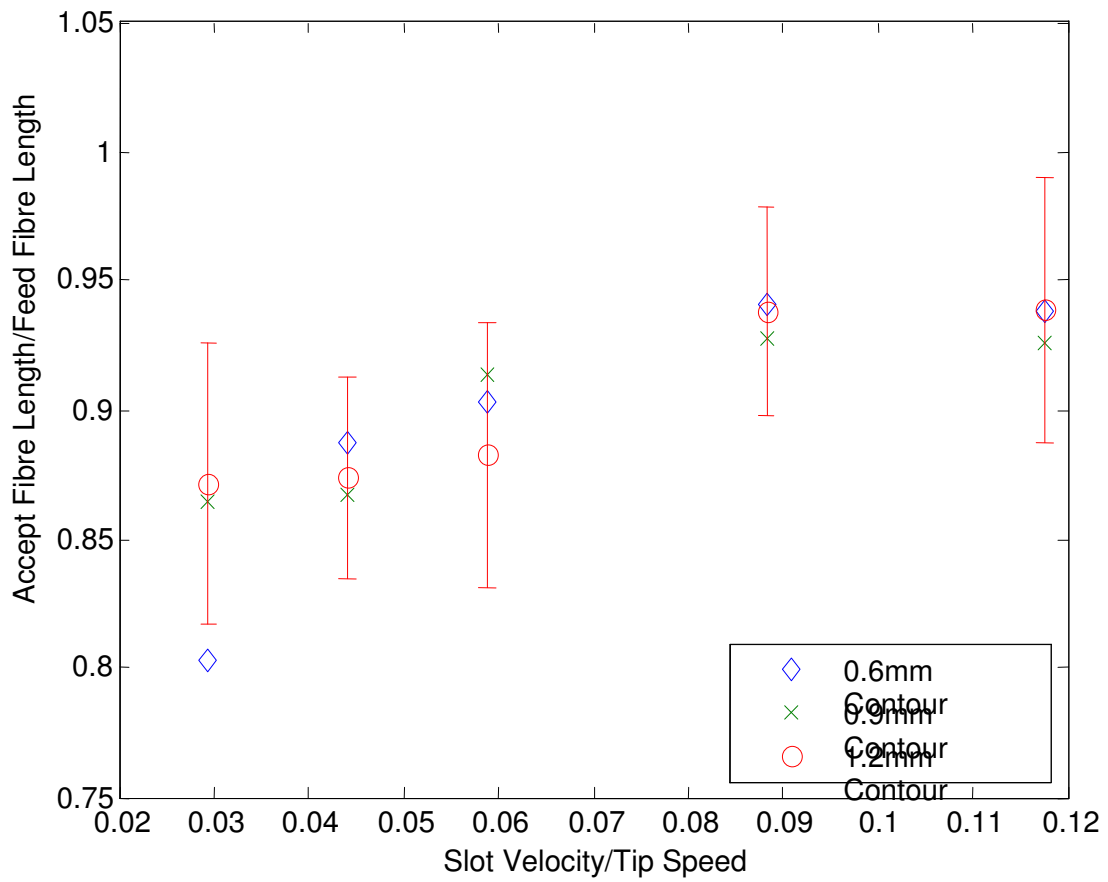


Figure B.5: Accept Fibre Length for 1.5% feed Consistency



. Figure B.6: Accept Fibre Length for 2.0% feed Consistency

APPENDIX C: COARSENESS

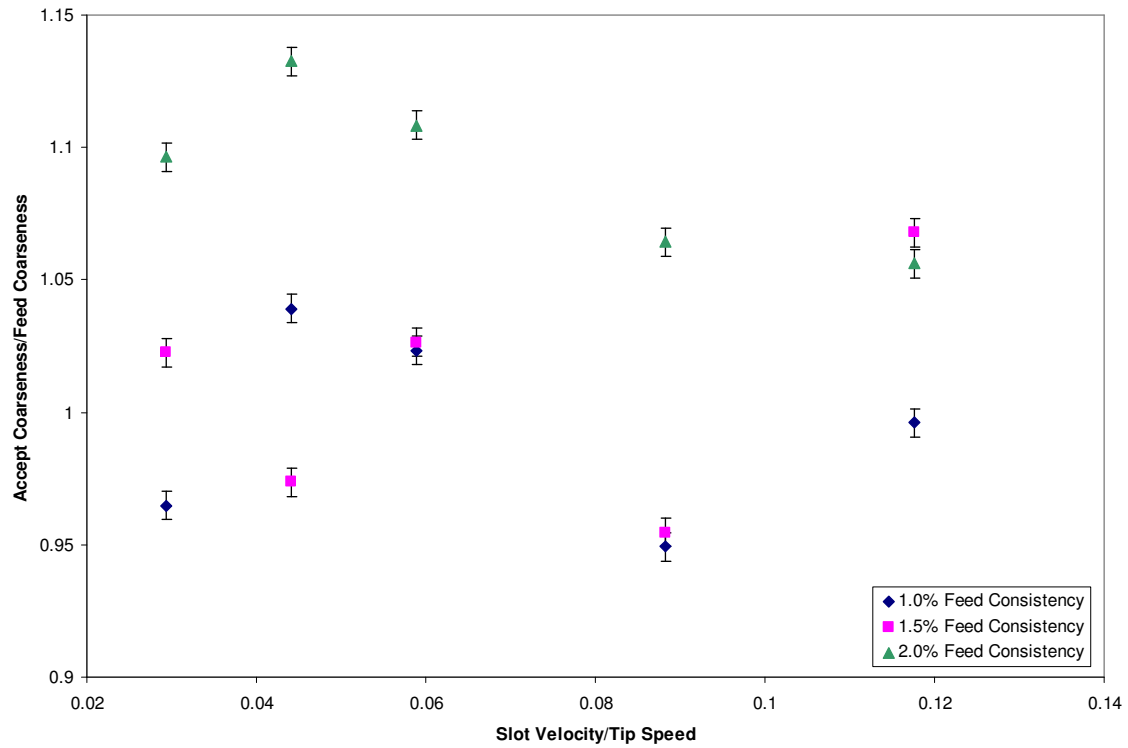


Figure C.1: Accept Coarseness vs. Slot Velocity
0.6mm Contour height.
FQA Error Bar=0.005

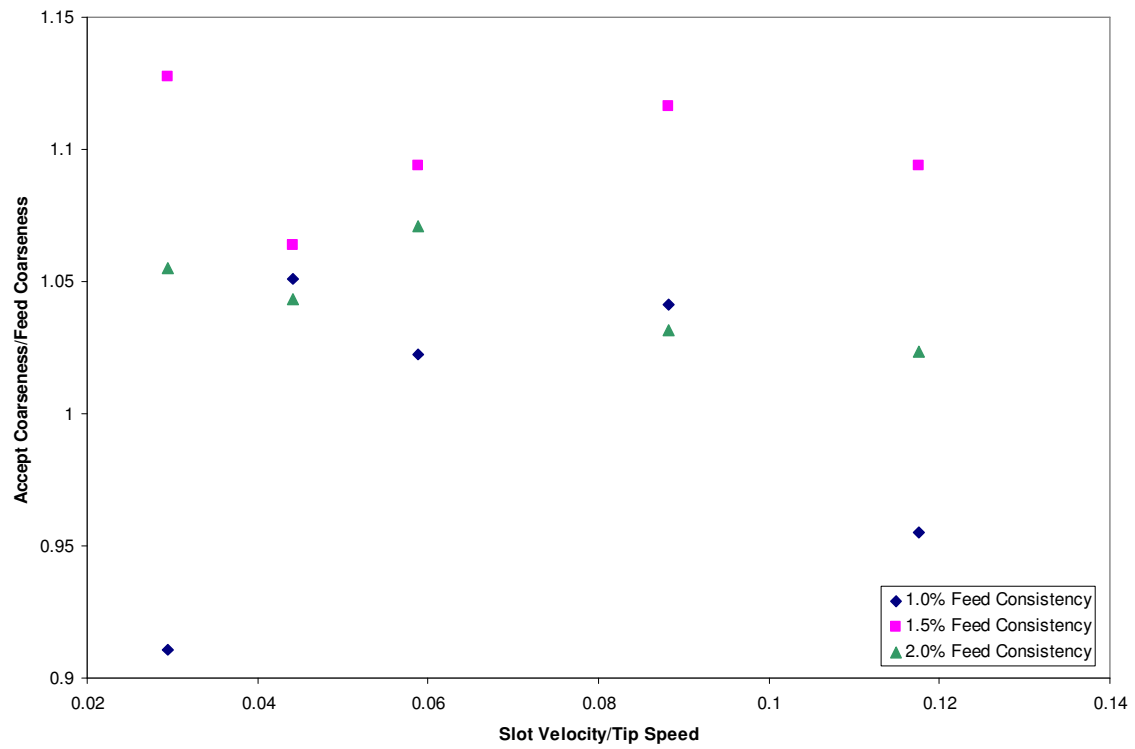


Figure C.2: Accept Coarseness vs. Slot Velocity
0.9mm Contour height.

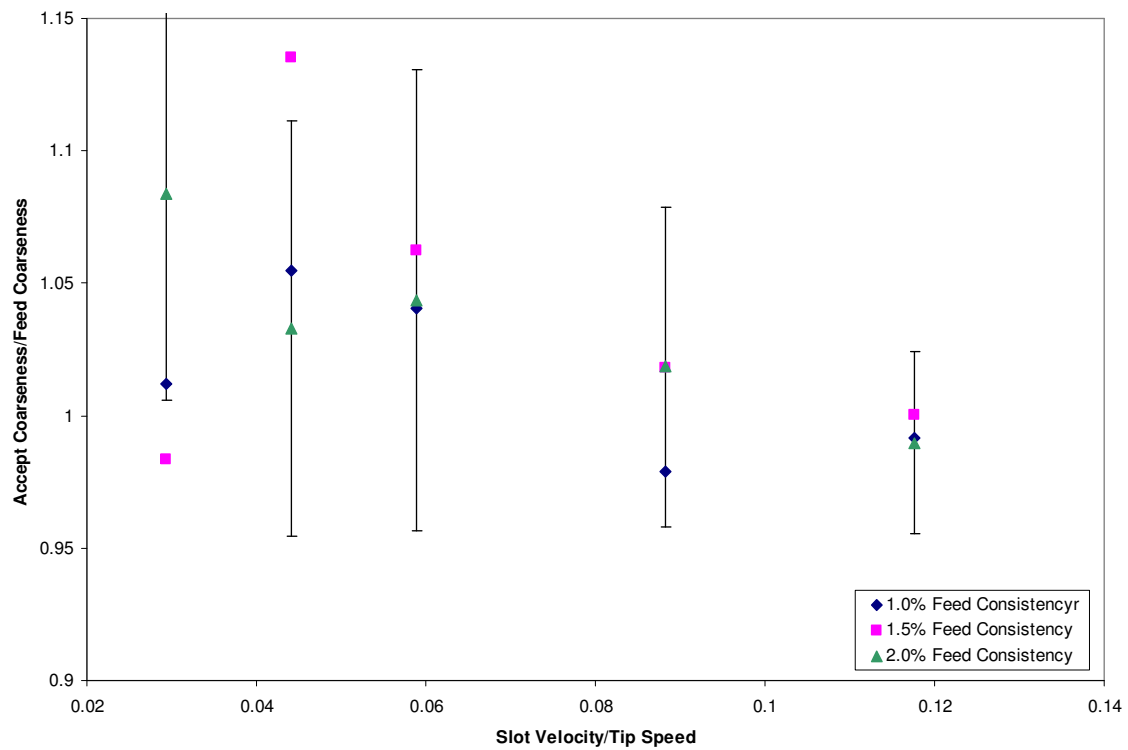


Figure C.3: Accept Coarseness vs. Slot Velocity
1.2mm Contour height. Experimental
Error Bars= 95% Confidence

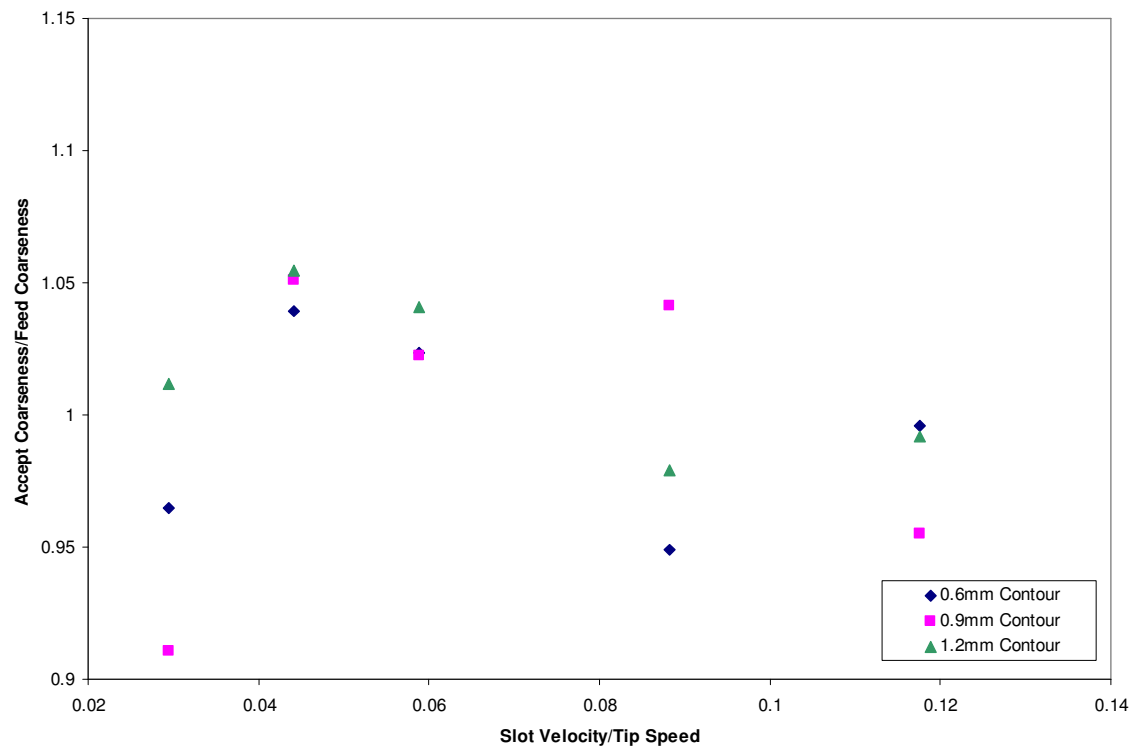


Figure C.4: Accept Coarseness vs. Slot Velocity
1.0% Feed Consistency.

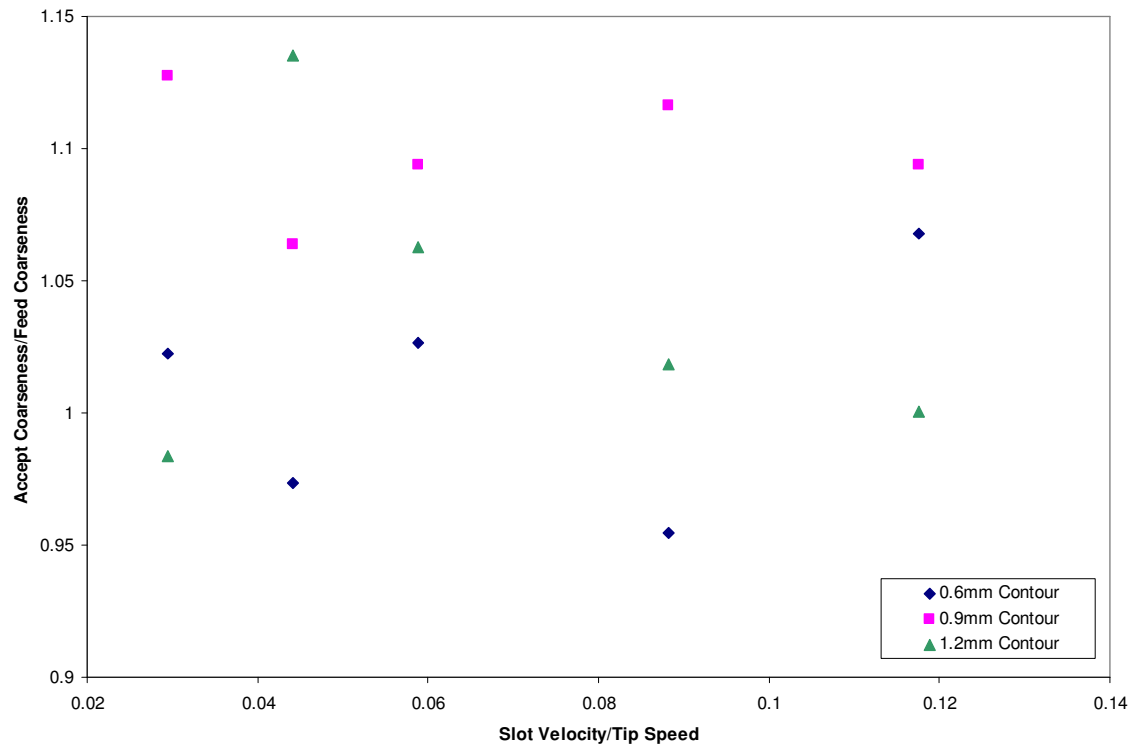


Figure C.5: Accept Coarseness vs. Slot Velocity
1.5% Feed Consistency.

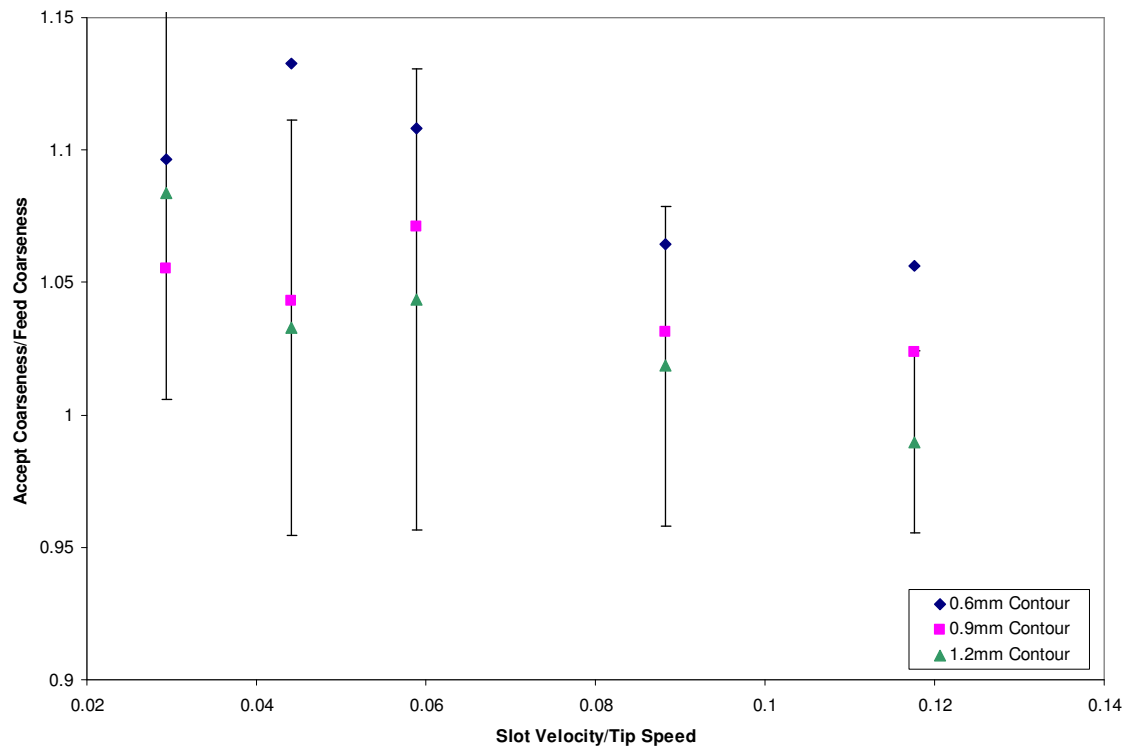


Figure C.6: Accept Coarseness vs. Slot Velocity
2.0% Feed Consistency.

APPENDIX D: EXPERIMENTAL RESULTS

Table D.1: Experimental Data for 1.0% feed consistency and 0.6mm Contour Height.

Pump Freq: 45 hz
 Screen: MF0632
 Open Area: 0.005824 m²
 Rotor RPM 1727.368
 TipSpeed 17 m/s
 Constant Rv 0.25
 Circumfrance 0.590494 m

Circumfrance 0.590494 m					Trial 1: 1.0% Feed Consistency													
Vs	Qa	Qr	Qf	Rotor Power KiloWatts	ACCEPT	ACCEPT	REJECT	REJECT	FEED	FEED	ACCEPT	REJECT	FEED	Consis A	Consis R	Consis F	Thicking	Passage
					LWLF	coarseness	LWLF	coarseness	LWLF	coarsenes	CSF	CSF	CSF					
(m/s)	(USGPM)	(USGPM)	(USGPM)		(mm)	mg/m	(mm)		(mm)		ml	ml	(ml)	%	%	%	-	
0.5	46.15614	15.38538	61.54152	4.55	1.269	0.247	1.78	0.245	1.474	0.256	75	335	129.5	0.006927	0.015632	0.009374	1.66759121	0.631117
0.75	69.23421	23.07807	92.31228	4.6	1.296	0.266	1.737	0.249	1.474	0.256	68	318	129.5	0.006545	0.0152905	0.009374	1.631160657	0.647051
1	92.31228	30.77076	123.083	4.5	1.309	0.262	1.713	0.263	1.474	0.256	75	310	129.5	0.006732	0.0150775	0.009374	1.608438233	0.65717
1.5	138.4684	46.15614	184.6246	4.3	1.406	0.243	1.595	0.258	1.474	0.256	86.5	236	129.5	0.008104	0.01419418	0.009522	1.490672076	0.712019
2	184.6246	61.54152	246.1661	4.25	1.442	0.255	1.622	0.243	1.474	0.256	102	184	129.5	0.008505	0.013351303	0.009522	1.402153253	0.756178
3	276.9368	92.31228	369.2491	2.8	1.452	0.246	1.578	0.265	1.474	0.256	110	181	129.5	0.00911	0.011502377	0.009522	1.207979104	0.863702

Table D.2: Experimental Data for 1.5% feed consistency and 0.6mm Contour Height

Pump Freq: 45 hz
 Screen: MF0632
 Open Area: 0.005824
 Rotor RPM 1727.368
 TipSpeed 17 m/s
 Constant Rv 0.254
 Circumfrance 0.590494 m

Circumfrance 0.590494 m				Trial 2.: 1.35-1.45% Feed Consistency																					
				ACCEPT		ACCEPT		REJECT		REJECT		FEED		FEED		ACCEPT		REJECT		FEED					
Vs	Qa	Qr	Qf	Rotor Power	LWLF	coarseness	LWLF	coarseness	LWLF	coarsenes	CSF	CSF	CSF	Consis A	Consis R	Consis F	Thicking	Passage							
(m/s)	(USGPM)	(USGPM)	(USGPM)	(Watts)	(mm)	mg/m	(mm)		(mm)		ml	ml	(ml)	%	%	%	-								
0.5	46.15614	15.38538	61.54152	4.8	1.279	0.271	1.691	0.239	1.474	0.265	71	395	136	0.00951	0.0235	0.0135	1.740740741	0.600149							
0.75	69.23421	23.07807	92.31228	4.9	1.289	0.258	1.677	0.249	1.474	0.265	82	355	136	0.010295	0.0227	0.0135	1.681481481	0.625134							
1	92.31228	30.77076	123.083	5	1.436	0.272	1.629	0.255	1.474	0.265	87	354	136	0.0105	0.0224	0.0135	1.659259259	0.63473							
1.5	138.4684	46.15614	184.6246	4.6	1.48	0.253	1.723	0.262	1.474	0.265	120	294	136	0.0117	0.0196	0.0139	1.410071942	0.752116							
2	184.6246	61.54152	246.1661	4.5	1.503	0.283	1.686	0.27	1.474	0.265	140	287	136	0.0127	0.0186	0.0139	1.338129496	0.789891							

Table D.3: Experimental Data for 2.0% feed consistency and 0.6mm Contour Height

Pump Freq: 45 hz
 Screen: MF0632
 Open Area: 0.005824
 Rotor RPM 1727.368
 TipSpeed 17 m/s
 Constant Rv 0.25
 Circumfrance 0.590494 m

Trial 3: 2.0% Feed Consistency

Vs (m/s)	Qa (USGPM)	Qr (USGPM)	Qf (USGPM)	Rotor Power (Watts)	ACCEPT	ACCEPT	REJECT	REJECT	FEED	FEED	ACCEPT	REJECT	FEED	Consis A %	Consis R %	Consis F %	Thickening -	Passage
					LWLF (mm)	coarseness mg/m	LWLF (mm)	coarseness	LWLF (mm)	coarseness	CSF ml	CSF ml	CSF (ml)					
0.5	46.15614	15.38538	61.54152	5.5	1.228	0.273	1.704	0.238	1.529	0.249	94	490	220	0.012593	0.032263	0.019324	1.669567	0.630263
0.75	69.23421	23.07807	92.31228	5.3	1.356	0.282	1.642	0.242	1.529	0.249	110	441	220	0.013756	0.033178	0.019324	1.716946	0.610078
1	92.31228	30.77076	123.083	6.3	1.381	0.276	1.639	0.247	1.529	0.249	124	426	220	0.014187	0.03018	0.019324	1.561801	0.678395
1.5	138.4684	46.15614	184.6246	6.6	1.439	0.265	1.672	0.247	1.529	0.249	139	397	220	0.015396	0.029155	0.019167	1.521131	0.697428
2	184.6246	61.54152	246.1661	4.9	1.434	0.263	1.64	0.252	1.529	0.249	153	349	220	0.016621	0.026948	0.019167	1.405987	0.754209
3	276.9368	92.31228	369.2491	3.5	1.532	0.244	1.634	0.251	1.529	0.249	177	270	220	0.017614	0.024991	0.019167	1.303868	0.808601

Table D.4: Experimental Data for 1.5% feed consistency and 0.6mm Contour Height

Pump Freq: 45 hz
 Screen: MF0632
 Open Area: 0.005824
 Rotor RPM 1727.368
 TipSpeed 17 m/s
 Constant Rv 0.5
 Circumfrance 0.590494 m

Trial 4: 1.5% Feed Consistency

Vs (m/s)	Qa (USGPM)	Qr (USGPM)	Qf (USGPM)	Rotor Power (KWatts)	ACCEPT	ACCEPT	REJECT	REJECT	FEED	FEED	ACCEPT	REJECT	FEED	Consis A %	Consis R %	Consis F %	Thickening -	Passage
					LWLF (mm)	coarseness mg/m	LWLF (mm)	coarseness	LWLF (mm)	coarseness	CSF ml	CSF ml	CSF (ml)					
0.5	46.15614	15.38538	61.54152	4.4	1.281	0.261	1.716	0.252	1.606	0.311	106	490	221	0.00981	0.024	0.01468	1.634877	0.645409
0.75	69.23421	23.07807	92.31228	4.2	1.288	0.278	1.661	0.229	1.606	0.311	113	441	221	0.0104	0.023	0.01468	1.566757	0.676109
1	92.31228	30.77076	123.083	4.2	1.326	0.264	1.672	0.267	1.606	0.311	N/A	423	221	0.0101	0.022	0.01468	1.498638	0.708174
1.5	138.4684	46.15614	184.6246	3.9	1.395	0.239	1.685	0.242	1.606	0.311	120	424	223	0.0114	0.021	0.01402	1.49786	0.708549
2	184.6246	61.54152	246.1661	3.7	1.412	0.265	1.624	0.231	1.606	0.311	140	346	223	0.0121	0.019	0.01402	1.355207	0.780743
3	276.9368	92.31228	369.2491	3.2	1.49	0.255	1.551	0.259	1.606	0.311	176	260	223	0.0136	0.0155	0.01402	1.105563	0.927609

Table D.5: Experimental Data for 2.0% feed consistency and 0.6mm Contour Height

Pump Freq: 45 hz
 Screen: MF0632
 Open Area: 0.005824
 Rotor RPM 1727.368
 TipSpeed 17 m/s
 Constant Rv 0.25
 Circumfrance 0.590494 m

Trial 5: 2.0% Feed Consistency																		
				ACCEPT		ACCEPT	REJECT	REJECT	FEED		FEED	ACCEPT	REJECT	FEED				
Vs	Qa	Qr	Qf	Rotor Power	LWLF	coarseness	LWLF	coarseness	LWLF	coarsenes	CSF	CSF	CSF	Consis A	Consis R	Consis F	Thicking	Passage
(m/s)	(USGPM)	(USGPM)	(USGPM)	(Watts)	(mm)	mg/m	(mm)		(mm)		ml	ml	(ml)	%	%	%	-	
0.5	46.15614	15.38538	61.54152	5.2	1.246	0.294	1.664	0.275	1.474	0.2872	55	298	135	0.01288	0.03661	0.02072	1.766891892	0.589393
0.75	69.23421	23.07807	92.31228	5	1.34	0.294	1.648	0.27	1.474	0.2872	64	275	135	0.01344	0.03532	0.02071	1.705456301	0.614921
1	92.31228	30.77076	123.083	4.9	1.411	0.288	1.639	0.252	1.474	0.2872	70	265	135	0.01484	0.0331	0.02071	1.598261709	0.661748
1.5	138.4684	46.15614	184.6246	4.5	1.429	0.302	1.62	0.278	1.474	0.2872	80	239	135	0.01623	0.03062	0.02071	1.478512796	0.717927
2	184.6246	61.54152	246.1661	4.1	1.473	0.279	1.562	0.265	1.474	0.2872	88	231	135	0.01692	0.02795	0.02071	1.34958957	0.78374
3	276.9368	92.31228	369.2491	Tried Twice could not attain these values.														

Table D.6: Experimental Data for 1.0% feed consistency and 0.9mm Contour Height

Pump Freq: 45 hz
Screen: MF0932
Open Area: 0.005824
Rotor RPM 1727.368
Tip Speed 17 m/s
Constant Rv 0.25
Circumference: 0.590494 m

Trial 1: 1.0% Feed Consistency

					ACCEPT	ACCEPT	REJECT	REJECT	FEED	FEED	ACCEPT	REJECT	FEED					
Vs	Qa	Qr	Qf	Rotor Power	LWLF	coarseness	LWLF	coarseness	LWLF	coarseness	CSF	CSF	CSF	Consis A	Consis R	Consis F	Thicking	Passage
(m/s)	(USGPM)	(USGPM)	(USGPM)	(KiloWatts)	(mm)	mg/m	(mm)		(mm)		ml	ml	(ml)	%	%	%	-	
0.5	46.15614	15.38538	61.54152	4.1	1.254	0.285	1.667	0.307	1.478	0.313	52	321	140	0.00638	0.0174	0.0109	1.59633	0.66262
0.75	69.23421	23.07807	92.31228	4	1.276	0.329	1.692	0.287	1.478	0.313	68	325	140	0.007625	0.01812	0.0109	1.662385	0.633373
1	92.31228	30.77076	123.083	3.9	1.274	0.32	1.681	0.26	1.478	0.313	66	306	140	0.007326	0.01679	0.0109	1.540367	0.688363
1.5	138.4684	46.15614	184.6246	3.8	1.319	0.326	1.716	0.272	1.478	0.313	78	259	140	0.00837	0.01566	0.0109	1.436697	0.738622
2	184.6246	61.54152	246.1661	3.7	1.449	0.299	1.593	0.257	1.478	0.313	95	235	140	0.008575	0.01417	0.0109	1.3	0.810744
3	276.9368	92.31228	369.2491															

Table D.7: Experimental Data for 1.5% feed consistency and 0.9mm Contour Height

Pump Freq: 45 hz
Screen: MF0932
Open Area: 0.005824
Rotor RPM 1727.368
Tip Speed 17 m/s
Constant Rv 0.25
Circumference: 0.590494 m

Trial 2 1.5% Feed Consistency

					ACCEPT	ACCEPT	REJECT	REJECT	FEED	FEED	ACCEPT	REJECT	FEED					
Vs	Qa	Qr	Qf	Rotor Power	LWLF	coarseness	LWLF	coarsenes	LWLF	coarsenes	CSF	CSF	CSF	Consis A	Consis R	Consis F	Thicking	Passage
(m/s)	(USGPM)	(USGPM)	(USGPM)	(Watts)	(mm)	mg/m	(mm)	mg/m	(mm)	mg/m	ml	ml	(ml)	%	%	%	-	
0.5	46.15614	15.38538	61.54152	4.6	1.272	0.301	1.668	0.258	1.51	0.267	52	321	129	0.0105	0.0314	0.0153	2.052288	0.481384
0.75	69.23421	23.07807	92.31228	4.4	1.306	0.284	1.647	0.267	1.51	0.267	54	278	129	0.0109	0.026227	0.0153	1.714183	0.611239
1	92.31228	30.77076	123.083	4.2	1.436	0.292	1.687	0.271	1.51	0.267	67	296	129	0.0116	0.0272	0.0153	1.777778	0.584963
1.5	138.4684	46.15614	184.6246	4.1	1.485	0.298	1.633	0.249	1.51	0.267	82	269	129	0.0135	0.02352	0.0153	1.537255	0.689822
2	184.6246	61.54152	246.1661	3.8	1.444	0.92	1.59	0.277	1.51	0.267	89	231	129	0.0132	0.024	0.0153	1.568627	0.675249
3	276.9368	92.31228	369.2491	3.33	1.513	0.275	1.5	0.257	1.51	0.267	109	186	129	0.0139	0.0184	0.0153	1.202614	0.866913

Table D.8: Experimental Data for 2.0% feed consistency and 0.9mm Contour Height

Pump Freq: 45 hz
Screen: MF0932
Open Area: 0.005824
Rotor RPM 1727.368
Tip Speed 17 m/s
Constant Rv 0.25
Circumference 0.590494 m

Trial 3: 2.0% Feed Consistency																		
ACCEPT		ACCEPT		REJECT		REJECT		FEED		FEED		ACCEPT		REJECT		FEED		
Vs	Qa	Qr	Qf	Rotor Power	LWLF	coarseness	LWLF	coarseness	LWLF	coarseness	CSF	CSF	CSF	Consis A	Consis R	Consis F	Thicking	Passage
(m/s)	(USGPM)	(USGPM)	(USGPM)	(Watts)	(mm)	mg/m	(mm)		(mm)		ml	ml	(ml)	%	%	%	-	
0.5	46.15614	15.38538	61.54152	4.9	1.278	0.268	1.696	0.238	1.479	0.254	47	290	137	0.0116	0.0352	0.0196	1.795918	0.577639
0.75	69.23421	23.07807	92.31228	4.6	1.282	0.265	1.662	0.243	1.479	0.254	51	276	137	0.01316	0.0321	0.0196	1.637755	0.64414
1	92.31228	30.77076	123.083	4.7	1.351	0.272	1.66	0.239	1.479	0.254	57	253	137	0.0123	0.0345	0.0196	1.760204	0.592129
1.5	138.4684	46.15614	184.6246	4.2	1.372	0.262	1.602	0.257	1.479	0.254	77	232	137	0.01536	0.0306	0.0196	1.561224	0.678661
2	184.6246	61.54152	246.1661	3.6	1.369	0.26	1.631	0.243	1.479	0.254	80	197	137	0.0164	0.027	0.0196	1.377551	0.768947
3	276.9368	92.31228	369.2491															

Table D.9: Experimental Data for 1.5% feed consistency and 0.9mm Contour Height

Pump Freq: 45 hz
Screen: MF0932
Open Area: 0.005824
Rotor RPM 1727.368
Tip Speed 17 m/s
Constant Rv 0.25
Circumference 0.590494 m

Trial 4: 1.5% Feed Consistency												
ACCEPT		REJECT		FEED								
Vs	Qa	Qr	Qf	Rotor Power	CSF	CSF	CSF	Consis A	Consis R	Consis F	Thicking	Passage
(m/s)	(USGPM)	(USGPM)	(USGPM)	(Watts)	ml	ml	(ml)	%	%	%	-	
0.5	46.15614	15.38538	61.54152	5.1	49.9	313.3	146	0.009898	0.028945	0.015981	1.81116	0.571543
0.75	69.23421	23.07807	92.31228		57.7	296.5	146	0.010174	0.026219	0.015981	1.640573	0.6429
1	92.31228	30.77076	123.083	4.8	69.5	283.1	146	0.012595	0.025443	0.015981	1.592047	0.664558
1.5	138.4684	46.15614	184.6246	4.5	88.4	264	146	0.010867	0.02375	0.015981	1.486111	0.714229
2	184.6246	61.54152	246.1661	4.2	92.7	232.5	146	0.013543	0.0217	0.015981	1.357836	0.779345
3	276.9368	92.31228	369.2491	Tried twice, could not reach these values								

Table D.10: Experimental Data for 1.0% feed consistency and 0.9mm Contour Height

Pump Freq: **45** hz
 Screen: **MF0932**
 Open Area: 0.005824
 Rotor RPM 1727.368
 Tip Speed 17 m/s
 Constant Rv 0.25
 Circumferenc 0.590494 m

Trial 5: 1.0% Feed Consistency

Vs	Qa	Qr	Qf	ACCEPT	REJECT	FEED	Consis A	Consis R	Consis F	Thicking	Passage
				CSF	CSF	CSF					
(m/s)	(USGPM)	(USGPM)	(USGPM)	ml	ml	(ml)	%	%	%	-	
0.5	46.15614	15.38538	61.54152	59.5	331	140	0.00693	0.01542	0.0101	1.5267327	0.694776
0.75	69.23421	23.07807	92.31228	62.2	315.3	140	0.006873	0.01603	0.0101	1.5871287	0.66679
1	92.31228	30.77076	123.083	70.2	289.9	140	0.00717	0.01514	0.0101	1.4990099	0.707995
1.5	138.4684	46.15614	184.6246	80.2	249.2	140	0.00803	0.0143	0.0101	1.4158416	0.74917
2	184.6246	61.54152	246.1661	90.8	228.2	140	0.0081	0.01384	0.0101	1.370297	0.772756
3	276.9368	92.31228	369.2491	Tried twice, could not reach these values							

Table D.11: Experimental Data for 1.0% feed consistency and 1.2mm Contour Height

Pump Freq: 45 hz
Screen: MF1232
Open Area: 0.005824
Rotor RPM 1727.367971
Tip Speed 17 m/s
Constant Rv 0.25
Circumference: 0.590493755 m

Trial 1: 1.0% Feed Consistency

Vs (m/s)	Qa (USGPM)	Qr (USGPM)	Qf (USGPM)	Rotor Power (Watts)	LWLF (mm)	ACCEPT	REJECT	REJECT	FEED	FEED	ACCEPT	REJECT	FEED	Consis A %	Consis R %	Consis F %	Thickening -	Passage
						coarseness mg/m	LWLF (mm)	coarseness	LWLF (mm)	coarseness	CSF ml	CSF ml	CSF (ml)					
0.5	46.15614093	15.38538	61.54152	4.1	1.417	0.302	1.722	0.258	1.502	0.267	159	422	245	0.00761	0.0146	0.00932	1.566524	0.676217
0.75	69.23421139	23.07807	92.31228	4.2	1.346	0.287	1.727	0.272	1.502	0.267	157	410	245	0.00763	0.014	0.00932	1.502146	0.706488
1	92.31228185	30.77076	123.083	3.9	1.433	0.3	1.7	0.292	1.502	0.267	165	388	245	0.00821	0.0137	0.00932	1.469957	0.722113
1.5	138.4684228	46.15614	184.6246	3.8	1.432	0.264	1.684	0.276	1.502	0.267	162	368	242	0.00804	0.0133	0.00978	1.359918	0.77824
2	184.6245637	61.54152	246.1661	3.7	1.455	0.282	1.596	0.252	1.502	0.267	183	296	242	0.00837	0.0119	0.00978	1.216769	0.858472
3	276.9368456	92.31228	369.2491	3.6	1.503	0.292			1.502	0.267	189	291	242	0.00841	0.0109	0.00978	1.114519	0.921789

Table D.12: Experimental Data for 1.5% feed consistency and 1.2mm Contour Height

Pump Freq: 45 hz
Screen: MF1232
Open Area: 0.005824
Rotor RPM 1727.368
Tip Speed 17 m/s
Constant Rv 0.25
Circumference 0.590494 m

Trial 2: 1.5% Feed Consistency

Vs (m/s)	Qa (USGPM)	Qr (USGPM)	Qf (USGPM)	Rotor Power (Watts)	LWLF (mm)	ACCEPT	REJECT	REJECT	FEED	FEED	ACCEPT	REJECT	FEED	Consis A %	Consis R %	Consis F %	Thickening -	Passage
						coarseness mg/m	LWLF (mm)	coarsenes mg/m	LWLF (mm)	coarsenes mg/m	CSF ml	CSF ml	CSF (ml)					
0.5	46.15614	15.38538	61.54152	4.4	1.335	0.247	1.684	0.228	1.528	0.244	122	484	338	0.009583	0.025	0.0154	1.623377	0.650501
0.75	69.23421	23.07807	92.31228	4.3	1.396	0.287	1.692	0.252	1.528	0.244	126	448	338	0.0111	0.0225	0.0154	1.461039	0.726503
1	92.31228	30.77076	123.083	4.2	1.442	0.27	1.62	0.259	1.528	0.244	136	427	338	0.0121	0.02099	0.0154	1.362987	0.776614
1.5	138.4684	46.15614	184.6246	4	1.441	0.241	1.628	0.264	1.528	0.244	156	410	338	0.0126	0.0211	0.0154	1.37013	0.772844
2	184.6246	61.54152	246.1661	3.8	1.472	0.268	1.638	0.241	1.528	0.244	175	353	338	0.0137	0.0188	0.0154	1.220779	0.856099
3	276.9368	92.31228	369.2491	3.4	1.452	0.225	1.614	0.258	1.528	0.244	189	300	338	0.0133	0.0172	0.0154	1.116883	0.920261

Table D.13: Experimental Data for 2.0% feed consistency and 1.2mm Contour Height

Pump Freq: 45 hz
Screen: MF1232
Open Area: 0.005824
Rotor RPM 1727.367971
Tip Speed 17 m/s
Constant Rv 0.25
Circumference: 0.590493755 m

Circumferenc: 0.590493755 m

Trial 3: 2.0% Feed Consistency																		
				ACCEPT	ACCEPT	REJECT	REJECT	FEED	FEED	ACCEPT	REJECT	FEED						
Vs	Qa	Qr	Qf	Rotor Power	LWLF	coarseness	LWLF	coarseness	LWLF	coarseness	CSF	CSF	CSF	Consis A	Consis R	Consis F	Thicking	Passage
(m/s)	(USGPM)	(USGPM)	(USGPM)	(Watts)	(mm)	mg/m	(mm)		(mm)		ml	ml	(ml)	%	%	%	-	
0.5	46.15614093	15.38538	61.54152	5	1.362	0.274	1.65	0.262	1.487	0.26	185	594	327	0.0125	0.03296	0.018	1.831111	0.56364
0.75	69.23421139	23.07807	92.31228	4.6	1.343	0.289	1.695	0.227	1.487	0.26	190	574	327	0.0121	0.0315	0.018	1.75	0.596323
1	92.31228185	30.77076	123.083	4.5	1.389	0.25	1.64	0.23	1.487	0.26	195	568	327	0.013	0.0302	0.018	1.677778	0.626724
1.5	138.4684228	46.15614	184.6246	4.2	1.431	0.253	1.673	0.228	1.487	0.26	212	541	327	0.014342	0.0278	0.018	1.544444	0.686456
2	184.6245637	61.54152	246.1661	4	1.464	0.262	1.619	0.244	1.487	0.26	273	495	327	0.0163	0.02582	0.018	1.434444	0.739754
3	276.9368456	92.31228	369.2491															

Table D.14: Experimental Data for 2.0% feed consistency and 1.2mm Contour Height

Screen: MF1232
Open Area: 0.005824
Rotor RPM 1727.368
Tip Speed 17 m/s
Constant Rv 0.25
Circumference: 0.590494 m

ACCEPT																			
ACCEPT						REJECT		REJECT		FEED		FEED		ACCEPT		REJECT		FEED	
Vs	Qa	Qr	Qf	Rotor Power	LWLF	coarseness	LWLF	coarseness	LWLF	coarseness	CSF	CSF	CSF	Consis A	Consis R	Consis F	Thicking	Passage	
(m/s)	(USGPM)	(USGPM)	(USGPM)	(Watts)	(mm)	mg/m	(mm)		(mm)		ml	ml	(ml)	%	%	%	-		
0.5	46.15614	15.38538	61.54152	5.2	1.333	0.284	1.696	0.263	1.537	0.268	174	593	325	0.0121	0.0335	0.0191	1.753927	0.594706	
0.75	69.23421	23.07807	92.31228	4.8	1.286	0.254	1.65	0.241	1.537	0.268	186	562	325	0.0135	0.0312	0.0191	1.633508	0.646013	
1	92.31228	30.77076	123.083	4.6	1.319	0.282	1.632	0.231	1.537	0.268	197	548	325	0.0143	0.0318	0.0191	1.664921	0.632273	
1.5	138.4684	46.15614	184.6246	4.3	1.387	0.289	1.645	0.244	1.537	0.268	211	510	325	0.01558	0.03	0.0191	1.570681	0.674305	
2	184.6246	61.54152	246.1661	4	1.409	0.27	1.6	0.265	1.537	0.268	245	475	325	0.0165	0.0279	0.0191	1.460733	0.726654	
3	276.9368	92.31228	369.2491																

Table D.15: Experimental Data for 2.0% feed consistency and 1.2mm Contour Height

Pump Freq: 45 hz
 Screen: MF1232
 Open Area: 0.005824
 Rotor RPM 1727.367971
 Tip Speed 17 m/s
 Constant Rv 0.25
 Circumferenc: 0.590493755 m

Trial 5: 2.0% Feed Consistency

Vs (m/s)	Qa (USGPM)	Qr (USGPM)	Qf (USGPM)	Rotor Power (Watts)	LWLF (mm)	ACCEPT coarseness mg/m	REJECT LWLF (mm)	coarseness	LWLF (mm)	FEED coarseness	ACCEPT CSF ml	REJECT CSF ml	FEED CSF (ml)	Consis A %	Consis R %	Consis F %	Thickening -	Passage
0.5	46.15614093	15.38538	61.54152	5.1	1.289	0.336	1.741	0.242	1.571	0.28	177	580	340	0.012566	0.033724	0.01856	1.817051	0.569201
0.75	69.23421139	23.07807	92.31228	4.9	1.393	0.305	1.695	0.26	1.571	0.28	187	567	340	0.013079	0.03093	0.01856	1.666527	0.631578
1	92.31228185	30.77076	123.083	4.7	1.338	0.326	1.691	0.358	1.571	0.28	208	553	340	0.013087	0.030864	0.01856	1.662981	0.633114
1.5	138.4684228	46.15614	184.6246	4.5	1.511	0.298	1.656	0.265	1.571	0.28	213	518	340	0.014841	0.029623	0.01856	1.596086	0.662731
2	184.6245637	61.54152	246.1661	4.1	1.416	0.282	1.625	0.283	1.571	0.28	254	481	340	0.015706	0.02605	0.01856	1.403612	0.755428
3	276.9368456	92.31228	369.2491															

Table D.16: Experimental Data for 1.0% feed consistency and 1.2mm Contour Height

Pump Freq: 45 hz
 Screen: MF1232
 Open Area: 0.005824
 Rotor RPM 1727.367971
 Tip Speed 17 m/s
 Constant Rv 0.25
 Circumferenc: 0.590493755 m

Trial 6: 1.0% Feed Consistency

Vs (m/s)	Qa (USGPM)	Qr (USGPM)	Qf (USGPM)	Rotor Power (Watts)	LWLF (mm)	ACCEPT coarseness mg/m	REJECT LWLF (mm)	coarseness	LWLF (mm)	FEED coarseness	ACCEPT CSF ml	REJECT CSF ml	FEED CSF (ml)	Consis A %	Consis R %	Consis F %	Thickening -	Passage
0.5	46.15614093	15.38538	61.54152	4.2	1.332	0.233	1.686	0.251	1.451	0.261	87	224	130	0.00772	0.0151	0.01024	1.474609	0.719834
0.75	69.23421139	23.07807	92.31228	4	1.408	0.27	1.718	0.233	1.451	0.261	90	247	130	0.00775	0.0154	0.01024	1.503906	0.705643
1	92.31228185	30.77076	123.083	3.9	1.384	0.25	1.632	0.258	1.451	0.261	88	225	130	0.00871	0.0136	0.01024	1.328125	0.795305
1.5	138.4684228	46.15614	184.6246	3.8	1.414	0.253	1.574	0.254	1.451	0.261	96	210	130	0.00882	0.0139	0.01024	1.357422	0.779565
2	184.6245637	61.54152	246.1661	3.7	1.435	0.242	1.659	0.253	1.451	0.261	91	195	130	0.00854	0.0129	0.01024	1.259766	0.833422
3	276.9368456	92.31228	369.2491	3.7	1.442	0.273	1.545	0.245	1.451	0.261	105	170	130	0.0091	0.0119	0.01024	1.162109	0.891627

Table D.17: Experimental Data for 1.5% feed consistency and 1.2mm Contour Height

Pump Freq: 45 hz
Screen: MF1232
Open Area: 0.005824
Rotor RPM 1727.367971
Tip Speed 17 m/s
Constant Rv 0.25
Circumferenc: 0.590493755 m

Trial 7: 1.5% Feed Consistency																		
Vs (m/s)	Qa (USGPM)	Qr (USGPM)	Qf (USGPM)	Rotor Power (Watts)	ACCEPT	ACCEPT	REJECT	REJECT	FEED	FEED	ACCEPT	REJECT	FEED	Consis A %	Consis R %	Consis F %	Thickening -	Passage
					LWLF (mm)	coarseness mg/m	LWLF (mm)	coarseness	LWLF (mm)	coarseness	CSF ml	CSF ml	CSF (ml)					
0.5	46.15614093	15.38538	61.54152	4.4	1.319	0.254	1.676	0.259	1.522	0.266	65	227	127	0.0119	0.0251	0.016	1.56875	0.675192
0.75	69.23421139	23.07807	92.31228	4.25	1.367	0.291	1.661	0.26	1.522	0.266	72	234	127	0.0109	0.02321	0.016	1.450625	0.731663
1	92.31228185	30.77076	123.083	4.2	1.375	0.271	1.685	0.251	1.522	0.266	76	230	127	0.012	0.0241	0.016	1.50625	0.704519
1.5	138.4684228	46.15614	184.6246	4	1.387	0.279	1.618	0.248	1.522	0.266	80	209	127	0.0122	0.0222	0.016	1.3875	0.763756
2	184.6245637	61.54152	246.1661	3.8	1.414	0.24	1.653	0.262	1.522	0.266	90	200	127	0.0129	0.0217	0.016	1.35625	0.780188
3	276.9368456	92.31228	369.2491															

Table D.18: Experimental Data for 1.0% feed consistency and 1.2mm Contour Height

Pump Freq: 45 hz
Screen: MF1232
Open Area: 0.005824
Rotor RPM 1727.367971
Tip Speed 17 m/s
Constant Rv 0.25
Circumferenc: 0.590493755 m

Trial 8: 2.0% Feed Consistency																		
Vs (m/s)	Qa (USGPM)	Qr (USGPM)	Qf (USGPM)	Rotor Power (Watts)	ACCEPT	ACCEPT	REJECT	REJECT	FEED	FEED	ACCEPT	REJECT	FEED	Consis A %	Consis R %	Consis F %	Thickening -	Passage
					LWLF (mm)	coarseness mg/m	LWLF (mm)	coarseness	LWLF (mm)	coarseness	CSF ml	CSF ml	CSF (ml)					
0.5	46.15614093	15.38538	61.54152	5.1	1.301	0.292	1.586	0.272	1.476	0.286	57	276	131	0.01266	0.0336	0.019	1.768421	0.588769
0.75	69.23421139	23.07807	92.31228	4.8	1.283	0.281	1.633	0.25	1.476	0.286	67	289	131	0.01315	0.0341	0.019	1.794737	0.578114
1	92.31228185	30.77076	123.083	4.6	1.308	0.285	1.656	0.264	1.476	0.286	65	253	131	0.01373	0.0301	0.019	1.584211	0.668118
1.5	138.4684228	46.15614	184.6246	4.2	1.368	0.274	1.637	0.26	1.476	0.286	74	226	131	0.01475	0.0277	0.019	1.457895	0.728057
2	184.6245637	61.54152	246.1661	4	1.406	0.268	1.645	0.247	1.476	0.286	79	206	131	0.01541	0.0257	0.019	1.352632	0.782116
3	276.9368456	92.31228	369.2491															

APPENDIX E: EXCEL WORK SHEETS

Table E.1: Passage Ratio Work Sheet for equation 5.2

	a	b	c	d	e	f	g	h				
	1.09222	-0.04784651	0.008533	0.068944	0.17761	0.052901	-0.132	0.010424				
Contour Height	Re	1/Re	c/rho	Rv	Vs/Vt	H/g	Ws/g	Ww/g	Passage	Pcalc	Diff sward	R-squared
1.00%	69863.69	1.4314E-05	9.44E-06	0.25	0.03	0.12	0.03	0.64	0.63	0.628523974	2.18E-06	0.7794084
	69863.69	1.4314E-05	9.44E-06	0.25	0.04	0.12	0.03	0.64	0.65	0.661473233	0.000132	
	69863.69	1.4314E-05	9.44E-06	0.25	0.06	0.12	0.03	0.64	0.66	0.710866299	0.002587	Sum Diff Sq
	69863.69	1.4314E-05	9.44E-06	0.25	0.09	0.12	0.03	0.64	0.71	0.763947609	0.00291	
	69863.69	1.4314E-05	9.44E-06	0.25	0.12	0.12	0.03	0.64	0.76	0.803996213	0.001936	0.16664752
	69863.69	1.4314E-05	9.44E-06	0.25	0.18	0.12	0.03	0.64	0.86	0.864031655	1.63E-05	
0.6mm	19864.75	5.034E-05	1.47E-05	0.25	0.03	0.12	0.03	0.64	0.65	0.610192343	0.001585	
1.50%	19864.75	5.034E-05	1.47E-05	0.25	0.04	0.12	0.03	0.64	0.68	0.642180599	0.00143	
	19864.75	5.034E-05	1.47E-05	0.25	0.06	0.12	0.03	0.64	0.71	0.690133059	0.000395	
	19864.75	5.034E-05	1.47E-05	0.25	0.09	0.12	0.03	0.64	0.71	0.741666191	0.001003	
	19864.75	5.034E-05	1.47E-05	0.25	0.12	0.12	0.03	0.64	0.78	0.780546731	2.99E-07	
	19864.75	5.034E-05	1.47E-05	0.25	0.18	0.12	0.03	0.64	0.93	0.83883117	0.008312	
	19864.75	5.034E-05	1.47E-05	0.25	0.03	0.12	0.03	0.64	0.6	0.610192343	0.000104	
	19864.75	5.034E-05	1.47E-05	0.25	0.04	0.12	0.03	0.64	0.63	0.642180599	0.000148	
	19864.75	5.034E-05	1.47E-05	0.25	0.06	0.12	0.03	0.64	0.63	0.690133059	0.003616	
	19864.75	5.034E-05	1.47E-05	0.25	0.09	0.12	0.03	0.64	0.75	0.741666191	6.95E-05	
	19864.75	5.034E-05	1.47E-05	0.25	0.12	0.12	0.03	0.64	0.79	0.780546731	8.94E-05	
2.00%	6745.3	0.00014825	1.01E-05	0.25	0.03	0.12	0.03	0.64	0.63	0.564519118	0.004288	
	6745.3	0.00014825	1.01E-05	0.25	0.04	0.12	0.03	0.64	0.61	0.594113035	0.000252	
	6745.3	0.00014825	1.01E-05	0.25	0.06	0.12	0.03	0.64	0.68	0.638476228	0.001724	
	6745.3	0.00014825	1.01E-05	0.25	0.09	0.12	0.03	0.64	0.7	0.686152077	0.000192	
	6745.3	0.00014825	1.01E-05	0.25	0.12	0.12	0.03	0.64	0.75	0.722122388	0.000777	
	6745.3	0.00014825	1.01E-05	0.25	0.18	0.12	0.03	0.64	0.81	0.776044205	0.001153	
	6745.3	0.00014825	1.01E-05	0.25	0.03	0.12	0.03	0.64	0.59	0.564519118	0.000649	
	6745.3	0.00014825	1.01E-05	0.25	0.04	0.12	0.03	0.64	0.61	0.594113035	0.000252	
	6745.3	0.00014825	1.01E-05	0.25	0.06	0.12	0.03	0.64	0.66	0.638476228	0.000463	
	6745.3	0.00014825	1.01E-05	0.25	0.09	0.12	0.03	0.64	0.72	0.686152077	0.001146	
	6745.3	0.00014825	1.01E-05	0.25	0.12	0.12	0.03	0.64	0.78	0.722122388	0.00335	
1.00%	49214.02	2.0319E-05	9.44E-06	0.25	0.03	0.18	0.03	0.64	0.66	0.631475859	0.000814	
	49214.02	2.0319E-05	9.44E-06	0.25	0.04	0.18	0.03	0.64	0.63	0.664579865	0.001196	
	49214.02	2.0319E-05	9.44E-06	0.25	0.06	0.18	0.03	0.64	0.69	0.714204908	0.000586	
	49214.02	2.0319E-05	9.44E-06	0.25	0.09	0.18	0.03	0.64	0.74	0.767535516	0.000758	
	49214.02	2.0319E-05	9.44E-06	0.25	0.12	0.18	0.03	0.64	0.81	0.80777221	4.96E-06	
	49214.02	2.0319E-05	9.44E-06	0.25	0.03	0.18	0.03	0.64	0.69	0.631475859	0.003425	
	49214.02	2.0319E-05	9.44E-06	0.25	0.04	0.18	0.03	0.64	0.67	0.664579865	2.94E-05	
	49214.02	2.0319E-05	9.44E-06	0.25	0.06	0.18	0.03	0.64	0.71	0.714204908	1.77E-05	
	49214.02	2.0319E-05	9.44E-06	0.25	0.09	0.18	0.03	0.64	0.75	0.767535516	0.000307	
	49214.02	2.0319E-05	9.44E-06	0.25	0.12	0.18	0.03	0.64	0.77	0.80777221	0.001427	
0.9mm	14382.19	6.953E-05	1.47E-05	0.25	0.03	0.18	0.03	0.64	0.48	0.613862709	0.017919	
1.50%	14382.19	6.953E-05	1.47E-05	0.25	0.04	0.18	0.03	0.64	0.61	0.646043378	0.001299	
	14382.19	6.953E-05	1.47E-05	0.25	0.06	0.18	0.03	0.64	0.58	0.694284276	0.013061	
	14382.19	6.953E-05	1.47E-05	0.25	0.09	0.18	0.03	0.64	0.69	0.746127385	0.00315	
	14382.19	6.953E-05	1.47E-05	0.25	0.12	0.18	0.03	0.64	0.68	0.785241795	0.011076	
	14382.19	6.953E-05	1.47E-05	0.25	0.18	0.18	0.03	0.64	0.87	0.843876821	0.000682	
	14382.19	6.953E-05	1.47E-05	0.25	0.03	0.18	0.03	0.64	0.57	0.613862709	0.001924	
	14382.19	6.953E-05	1.47E-05	0.25	0.04	0.18	0.03	0.64	0.64	0.646043378	3.65E-05	
	14382.19	6.953E-05	1.47E-05	0.25	0.06	0.18	0.03	0.64	0.66	0.694284276	0.001175	
	14382.19	6.953E-05	1.47E-05	0.25	0.09	0.18	0.03	0.64	0.71	0.746127385	0.001305	
	14382.19	6.953E-05	1.47E-05	0.25	0.12	0.18	0.03	0.64	0.78	0.785241795	2.75E-05	
2.00%	7177.56	0.00013932	1.01E-05	0.25	0.03	0.18	0.03	0.64	0.58	0.578475137	2.33E-06	
	7177.56	0.00013932	1.01E-05	0.25	0.04	0.18	0.03	0.64	0.64	0.608800674	0.000973	
	7177.56	0.00013932	1.01E-05	0.25	0.06	0.18	0.03	0.64	0.59	0.654260612	0.004129	
	7177.56	0.00013932	1.01E-05	0.25	0.09	0.18	0.03	0.64	0.68	0.703115102	0.000534	
	7177.56	0.00013932	1.01E-05	0.25	0.12	0.18	0.03	0.64	0.77	0.739974669	0.000902	

1.00%	61274.88	1.632E-05	9.44E-06	0.25	0.03	0.24	0.03	0.64	0.68	0.647919105	0.001029	
	61274.88	1.632E-05	9.44E-06	0.25	0.04	0.24	0.03	0.64	0.71	0.681885119	0.00079	
	61274.88	1.632E-05	9.44E-06	0.25	0.06	0.24	0.03	0.64	0.72	0.732802367	0.000164	
	61274.88	1.632E-05	9.44E-06	0.25	0.09	0.24	0.03	0.64	0.78	0.787521672	5.66E-05	
	61274.88	1.632E-05	9.44E-06	0.25	0.12	0.24	0.03	0.64	0.86	0.828806105	0.000973	
	61274.88	1.632E-05	9.44E-06	0.25	0.18	0.24	0.03	0.64	0.92	0.890694133	0.000859	
	61274.88	1.632E-05	9.44E-06	0.25	0.03	0.24	0.03	0.64	0.72	0.647919105	0.005196	
	61274.88	1.632E-05	9.44E-06	0.25	0.04	0.24	0.03	0.64	0.71	0.681885119	0.00079	
	61274.88	1.632E-05	9.44E-06	0.25	0.06	0.24	0.03	0.64	0.8	0.732802367	0.004516	
	61274.88	1.632E-05	9.44E-06	0.25	0.09	0.24	0.03	0.64	0.78	0.787521672	5.66E-05	
	61274.88	1.632E-05	9.44E-06	0.25	0.12	0.24	0.03	0.64	0.83	0.828806105	1.43E-06	
	61274.88	1.632E-05	9.44E-06	0.25	0.18	0.24	0.03	0.64	0.89	0.890694133	4.82E-07	
1.2mm	14216.77	7.0339E-05	1.47E-05	0.25	0.03	0.24	0.03	0.64	0.68	0.622931393	0.003257	
1.50%	14216.77	7.0339E-05	1.47E-05	0.25	0.04	0.24	0.03	0.64	0.73	0.655587471	0.005537	
	14216.77	7.0339E-05	1.47E-05	0.25	0.06	0.24	0.03	0.64	0.7	0.704541039	2.06E-05	
	14216.77	7.0339E-05	1.47E-05	0.25	0.09	0.24	0.03	0.64	0.76	0.757150034	8.12E-06	
	14216.77	7.0339E-05	1.47E-05	0.25	0.12	0.24	0.03	0.64	0.78	0.796842288	0.000284	
	14216.77	7.0339E-05	1.47E-05	0.25	0.03	0.24	0.03	0.64	0.65	0.622931393	0.000733	
	14216.77	7.0339E-05	1.47E-05	0.25	0.04	0.24	0.03	0.64	0.73	0.655587471	0.005537	
	14216.77	7.0339E-05	1.47E-05	0.25	0.06	0.24	0.03	0.64	0.78	0.704541039	0.005694	
	14216.77	7.0339E-05	1.47E-05	0.25	0.09	0.24	0.03	0.64	0.77	0.757150034	0.000165	
	14216.77	7.0339E-05	1.47E-05	0.25	0.12	0.24	0.03	0.64	0.86	0.796842288	0.003989	
	14216.77	7.0339E-05	1.47E-05	0.25	0.18	0.24	0.03	0.64	0.92	0.856343536	0.004052	
2.00%	8344.42	0.00011984	1.01E-05	0.25	0.03	0.24	0.03	0.64	0.59	0.591594509	2.54E-06	
	8344.42	0.00011984	1.01E-05	0.25	0.04	0.24	0.03	0.64	0.58	0.622607807	0.001815	
	8344.42	0.00011984	1.01E-05	0.25	0.06	0.24	0.03	0.64	0.67	0.66909874	8.12E-07	
	8344.42	0.00011984	1.01E-05	0.25	0.09	0.24	0.03	0.64	0.73	0.719061213	0.00012	
	8344.42	0.00011984	1.01E-05	0.25	0.12	0.24	0.03	0.64	0.78	0.756756727	0.00054	
	8344.42	0.00011984	1.01E-05	0.25	0.03	0.24	0.03	0.64	0.57	0.591594509	0.000466	
	8344.42	0.00011984	1.01E-05	0.25	0.04	0.24	0.03	0.64	0.63	0.622607807	5.46E-05	
	8344.42	0.00011984	1.01E-05	0.25	0.06	0.24	0.03	0.64	0.63	0.66909874	0.001529	
	8344.42	0.00011984	1.01E-05	0.25	0.09	0.24	0.03	0.64	0.66	0.719061213	0.003488	
	8344.42	0.00011984	1.01E-05	0.25	0.12	0.24	0.03	0.64	0.76	0.756756727	1.05E-05	
	8344.42	0.00011984	1.01E-05	0.25	0.03	0.24	0.03	0.64	0.59	0.591594509	2.54E-06	
	8344.42	0.00011984	1.01E-05	0.25	0.04	0.24	0.03	0.64	0.65	0.622607807	0.00075	
	8344.42	0.00011984	1.01E-05	0.25	0.06	0.24	0.03	0.64	0.63	0.66909874	0.001529	
	8344.42	0.00011984	1.01E-05	0.25	0.09	0.24	0.03	0.64	0.67	0.719061213	0.002407	
	8344.42	0.00011984	1.01E-05	0.25	0.12	0.24	0.03	0.64	0.73	0.756756727	0.000716	
	8344.42	0.00011984	1.01E-05	0.25	0.03	0.24	0.03	0.64	0.56	0.591594509	0.000998	
	8344.42	0.00011984	1.01E-05	0.25	0.04	0.24	0.03	0.64	0.6	0.622607807	0.000511	
	8344.42	0.00011984	1.01E-05	0.25	0.06	0.24	0.03	0.64	0.63	0.66909874	0.001529	
	8344.42	0.00011984	1.01E-05	0.25	0.09	0.24	0.03	0.64	0.69	0.719061213	0.000845	
	8344.42	0.00011984	1.01E-05	0.25	0.12	0.24	0.03	0.64	0.74	0.756756727	0.000281	

Table E.2: Passage Ratio Work Sheet for equation 5.3

ASSUME EQUATION IS FORM $P=(V_s/V_t)^b$ $b \leq 1$ $b=f(H/W, C/\rho)$					
Contour Height	V_s/V_t	Passage(P)	b	P	R-squared
1.0%	0.029411765	0.63111716	0.132521	0.626681	0.908656
	0.044117647	0.64705056		0.661275	
	0.058823529	0.65716973		0.686972	
	0.088235294	0.71201854		0.724895	
	0.117647059	0.75617798		0.753064	
	0.176470588	0.86370225		0.794635	
0.6mm 1.5%	0.029411765	0.64540878	0.12787	0.637044	0.848689
	0.044117647	0.67610905		0.670944	
	0.058823529	0.70817422		0.696085	
	0.088235294	0.70854851		0.733126	
	0.117647059	0.78074347		0.760597	
	0.176470588	0.92760907		0.801072	
	0.029411765	0.60014933		0.637044	
	0.044117647	0.62513355		0.670944	
	0.058823529	0.63473034		0.696085	
	0.088235294	0.75211561		0.733126	
	0.117647059	0.78989113		0.760597	
2.0%	0.029411765	0.630263	0.141067	0.608077	0.925681
	0.044117647	0.61007757		0.643871	
	0.058823529	0.6783949		0.670539	
	0.088235294	0.69742785		0.71001	
	0.117647059	0.75420858		0.739417	
	0.176470588	0.80860117		0.782943	
	0.029411765	0.58939311		0.608077	
	0.044117647	0.61492111		0.643871	
	0.058823529	0.66174817		0.670539	
	0.088235294	0.71792664		0.71001	
	0.117647059	0.78373964		0.739417	
1.0%	0.029411765	0.66262041	0.119885	0.655237	0.744969
	0.044117647	0.63337259		0.687874	
	0.058823529	0.68836295		0.712012	
	0.088235294	0.73862196		0.747477	
	0.117647059	0.81074419		0.773707	
	0.029411765	0.69477626		0.655237	
	0.044117647	0.66679043		0.687874	
	0.058823529	0.70799504		0.712012	
	0.088235294	0.74917007		0.747477	
	0.117647059	0.77275568		0.773707	
0.9mm 1.5%	0.029411765	0.48138355	0.155811	0.577271	0.82475

		0.044117647	0.61123943		0.614917	
		0.058823529	0.5849625		0.643107	
		0.088235294	0.6898218		0.685046	
		0.117647059	0.67524862		0.716451	
		0.176470588	0.86691294		0.763174	
		0.029411765	0.57154316		0.577271	
		0.044117647	0.64290019		0.614917	
		0.058823529	0.66455837		0.643107	
		0.088235294	0.71422901		0.685046	
		0.117647059	0.77934524		0.716451	
2.0%		0.029411765	0.57763911	0.153742	0.581496	0.763834
		0.044117647	0.64414018		0.618899	
		0.058823529	0.59212865		0.646886	
		0.088235294	0.678661		0.688495	
		0.117647059	0.76894712		0.71963	
1.0%		0.029411765	0.67621675	0.096275	0.712125	0.891538
		0.044117647	0.70648752		0.740474	
		0.058823529	0.72211298		0.761269	
		0.088235294	0.77824006		0.791574	
		0.117647059	0.8584724		0.813804	
		0.176470588	0.92178912		0.8462	
		0.029411765	0.71983358		0.712125	
		0.044117647	0.70564268		0.740474	
		0.058823529	0.79530453		0.761269	
		0.088235294	0.77956542		0.791574	
		0.117647059	0.83342232		0.813804	
		0.176470588	0.89162707		0.8462	
1.2mm 1.5%		0.029411765	0.67519227	0.103679	0.693773	0.841486
		0.044117647	0.73166269		0.72356	
		0.058823529	0.70451938		0.745466	
		0.088235294	0.76375611		0.777473	
		0.117647059	0.78018843		0.801011	
		0.029411765	0.65050113		0.693773	
		0.044117647	0.72650267		0.72356	
		0.058823529	0.77661409		0.745466	
		0.088235294	0.77284368		0.777473	
		0.117647059	0.85609884		0.801011	
		0.176470588	0.92026089		0.835402	
2.0%		0.029411765	0.58876909	0.152628	0.583787	0.866587
		0.044117647	0.57811384		0.621056	
		0.058823529	0.66811797		0.648933	
		0.088235294	0.72805672		0.690361	
		0.117647059	0.78211553		0.721348	
		0.029411765	0.56920071		0.583787	
		0.044117647	0.63157771		0.621056	
		0.058823529	0.63311399		0.648933	

	0.088235294	0.66273098		0.690361	
	0.117647059	0.75542781		0.721348	
	0.029411765	0.59470577		0.583787	
	0.044117647	0.6460133		0.621056	
	0.058823529	0.63227294		0.648933	
	0.088235294	0.67430507		0.690361	
	0.117647059	0.72665376		0.721348	
	0.029411765	0.56364033		0.583787	
	0.044117647	0.59632254		0.621056	
	0.058823529	0.62672418		0.648933	
	0.088235294	0.68645601		0.690361	
	0.117647059	0.73975395		0.721348	

Table E.3: Accept Freeness Work Sheet for equation in figure 5.3

Contour Height	Slot Velocity	Passage Ratio	Acc Freeness	a	b	Calc Free	Rsqr
1.0%	0.0294	0.6311	0.5792	1.0508	1.5250	0.5208	0.64
	0.0441	0.6471	0.5251			0.5410	
	0.0588	0.6572	0.5792			0.5540	
	0.0882	0.7120	0.6680			0.6260	
	0.1176	0.7562	0.7876			0.6862	
	0.1765	0.8637	0.8494			0.8404	
0.6mm 1.5%	0.0294	0.6001	0.5221			0.4824	
	0.0441	0.6251	0.6029			0.5133	
	0.0588	0.6347	0.6397			0.5254	
	0.0882	0.7521	0.8824			0.6805	
	0.1176	0.7899	1.0294			0.7333	
2.0%	0.0294	0.5894	0.4074			0.4692	
	0.0441	0.6149	0.4741			0.5006	
	0.0588	0.6617	0.5185			0.5599	
	0.0882	0.7179	0.5926			0.6339	
	0.1176	0.7837	0.6519			0.7247	
1.0%	0.0294	0.6626	0.6626			0.5610	
	0.0441	0.6334	0.6334			0.5237	
	0.0588	0.6884	0.6884			0.5946	
	0.0882	0.7386	0.7386			0.6620	
	0.1176	0.8107	0.8107			0.7631	
0.9mm 1.5%	0.0294	0.4814	0.4031			0.3446	
	0.0441	0.6112	0.4186			0.4960	
	0.0588	0.5850	0.5194			0.4639	
	0.0882	0.6898	0.6357			0.5965	
	0.1176	0.6752	0.6899			0.5774	
	0.1765	0.8669	0.8450			0.8452	
	0.0294	0.5715	0.3418			0.4477	
	0.0441	0.6429	0.3952			0.5357	
	0.0588	0.6646	0.4760			0.5635	
	0.0882	0.7142	0.6055			0.6290	
	0.1176	0.7793	0.6349			0.7185	
2.0%	0.0294	0.5776	0.3431			0.4550	
	0.0441	0.6441	0.3723			0.5373	
	0.0588	0.5921	0.4161			0.4726	
	0.0882	0.6787	0.5620			0.5818	
	0.1176	0.7689	0.5839			0.7039	
1.0%	0.0294	0.7198	0.6692			0.6365	
	0.0441	0.7056	0.6923			0.6175	
	0.0588	0.7953	0.6769			0.7410	
	0.0882	0.7796	0.7385			0.7188	

	0.1176	0.8334	0.7000			0.7959	
	0.1765	0.8916	0.8077			0.8822	
1.2mm 1.5%	0.0294	0.6752	0.5118			0.5773	
	0.0441	0.7317	0.5669			0.6525	
	0.0588	0.7045	0.5984			0.6160	
	0.0882	0.7638	0.6299			0.6967	
	0.1176	0.7802	0.7087			0.7197	
2.0%	0.0294	0.5636	0.4351			0.4383	
	0.0441	0.5963	0.5115			0.4777	
	0.0588	0.6267	0.4962			0.5153	
	0.0882	0.6865	0.5649			0.5920	
	0.1176	0.7398	0.6031			0.6636	

Table E.4: Comparison of Equation 5.4 with actual data.

B	Calc Freeness	Act. Freeness	Rsqr
0.132521	0.507332256	0.5792	0.865538
	0.551973353	0.5251	
	0.586009174	0.5792	
	0.637573198	0.6680	
	0.676887283	0.7876	
	0.736447838	0.8494	
0.12787	0.520561445	0.5221	0.947248
	0.564692736	0.6029	
	0.598255189	0.6397	
	0.64897307	0.8824	
	0.687544715	1.0294	
0.141067	0.483894969	0.4074	0.99965
	0.529344755	0.4741	
	0.564157923	0.5185	
	0.617146399	0.5926	
	0.657733976	0.6519	
0.119885	0.544083311	0.6626	0.822686
	0.587217143	0.6334	
	0.619879382	0.6884	
	0.669022176	0.7386	
	0.706234581	0.8107	
0.155811	0.445978027	0.4031	0.954432
	0.492465297	0.4186	
	0.528358536	0.5194	
	0.583432877	0.6357	
	0.62595627	0.6899	
	0.691203875	0.8450	
	0.445978027	0.3418	
	0.492465297	0.3952	
	0.528358536	0.4760	
	0.583432877	0.6055	
	0.62595627	0.6349	
0.153742	0.451112669	0.3431	0.940585
	0.497479922	0.3723	
	0.533240432	0.4161	
	0.588049121	0.5620	
	0.630320046	0.5839	
0.096275	0.620033944	0.6692	0.69745
	0.659209713	0.6923	
	0.688497501	0.6769	
	0.731999022	0.7385	

	0.764520739	0.7000	
	0.812825656	0.8077	
0.103679	0.59514027	0.5118	0.964152
	0.635731439	0.5669	
	0.66619946	0.5984	
	0.711637177	0.6299	
	0.74574305	0.7087	
0.152628	0.453904262	0.4351	0.928647
	0.500203507	0.5115	
	0.535890025	0.4962	
	0.590552001	0.5649	
	0.632684341	0.6031	

APPENDIX F: PULP QUALITY

Manual: Technical Procedures Manual
Procedure Title: Pulp Evaluation Request Form
Procedure No. TPM - F
Owner: Technical Manager

Date Effective: 02/26/03
Rev. No.: 5.0
Page 1 of 2

PULP EVALUATION REQUEST FORM

Sample ID: <u>EW-649</u>	
Date Requested: _____	Requested By: _____
Basis Weight for Handsheets: _____	Disintegration Time: _____
Priority: Immediate: <input type="checkbox"/>	No Rush: <input type="checkbox"/>
Authorized By: _____	

Test	Requested Yes/No	Done Initial	Results
Species (%)			
CSF	13.1		
Brightness (457 ISO)	64.2		
Opacity (%)	92.7		
S (Cm ² /g)	52.5		
K (Cm ² /g)	2.33		
Color (L*a*b*)			
pH	8.9		
Basis Weight (g/m ²)			
Bulk (CC/g)	2.48		
Tear (mN.m ² /g)	9.5		
Burst (kPa.m ² /g)	2.4		
Breaking Length (km)	4.3		
TEA (mJ/g)	771		
Sclereids (count)			
Britt Jar Fines (%)			
Pulmac 0.006 (%)	.012		
Pulmac 0.004 (%)			
LWFL (mm)	1.51		
WWFL (mm)	2.27		

+3 (%)		11.3		
3/2 (%)		20.2		
2/1 (%)		28.2		
1/0.5 (%)		18.2		
-0.5 (%)		22.1		
Coarseness (mg/m)				
PPS (Smoothness) (microns)				
Gurley (Porosity) (sec/100ml)				
Bound Sulphur (%)				
SiO ₂ (%)				
COD/BOD (kg/ton)				
Ash @ 525°C (%)				
Extractives	DCM (%)			
- Must be fresh or frozen	Hot Water (%)			
Taber Stiffness (g.cm)				
Scott Bond (ft-lb 0.001)				
Fold (count)				

Copies to: _____ (To be filled out by person requesting tests).

Tester: _____

Date: _____

APPENDIX G: ERROR ANALYSIS

Propagation error slot velocity:

$$V_s = \frac{Q}{A}$$

$$\Delta V_s = \frac{d}{dQ} \left(\frac{Q}{A} \right) \times \Delta Q + \frac{d}{dA} \left(\frac{Q}{A} \right) \times \Delta A$$

$$\Delta V_s = \frac{\Delta Q}{A} + \frac{n l Q}{n^2 l^2} \times \frac{d}{dw} \left(\frac{1}{w} \right) \times \Delta w$$

$$\Delta V_s = \frac{\Delta Q}{A} - \frac{Q}{A^2} \times \Delta A$$

V_s = Slot Velocity
A = Open Area
n = # of Slots
Q = Flowrate
l = Screen length
w = Slot width
ΔV_s = Change in slot Velocity
ΔQ = Change in flow Rate

Error in Fitting Parameter B: eqn 5.3

All work was done on excel sheet. Below is the general method that I used. Used a matrix approach to solve the error and develop a confidence.

$$\{A\} = \left[[Z]^T [Z] \right]^{-1} \times \{ [Z]^T [Y] \}$$

A = Contains Unknown Coefficients
 Z = calculated values of z function of independent variables
 Y = Observed values of dependent variables

The diagonal and off-diagonal terms of the matrix $\left[[Z]^T [Z] \right]^{-1}$ give the variances and covariances of unknown coefficients. Then the standard error calculated from

$$s(a_i) = \sqrt{Z_{ii}^{-1} s_{y/x}^2}$$

$$s_{y/x} = \sqrt{\frac{Sr}{n-2}}$$

$$Sr = \sum_{i=1}^n (y_i - \bar{y})^2$$

Z_{ii} = Diagonal Elements

$S_{y/x}$ = Standard Error of the estimate

Sr = Sum squared differences

Then using t distributions you can determine 95% confidence interval.

Table G.1: Error analysis of fitting parameter B.

ln(passage)	Ln(vs/vt)	Z ⁻¹	s ² y/x	s=	tin _v	tin _v *s
-0.46026375	-3.52636	0.0229	0.001211	0.034802067	2.570582	0.089462
-0.43533085	-3.1209					
-0.41981295	-2.83321					
-0.33965133	-2.42775					
-0.27947851	-2.14007					
-0.14652719	-1.7346	0.0119	0.002856	0.053444808	2.262157	0.120901
-0.43787139	-3.52636					
-0.39140089	-3.1209					
-0.34506514	-2.83321					
-0.34453675	-2.42775					
-0.24750865	-2.14007					
-0.0751449	-1.7346					
-0.51057678	-3.52636					
-0.46978996	-3.1209					
-0.45455504	-2.83321					
-0.28486522	-2.42775	0.0119	0.000602	0.024541945	2.228139	0.054683
-0.23586015	-2.14007					
-0.46161808	-3.52636					
-0.49416917	-3.1209					
-0.3880257	-2.83321					
-0.36035621	-2.42775					
-0.28208631	-2.14007					
-0.21244948	-1.7346					
-0.52866189	-3.52636					
-0.4862613	-3.1209					
-0.41287021	-2.83321					
-0.33138789	-2.42775					
-0.24367841	-2.14007					
-0.41155298	-3.52636	0.0123	0.000937	0.030610603	2.262157	0.069246
-0.45669642	-3.1209					
-0.37343903	-2.83321					
-0.30296904	-2.42775					
-0.2098027	-2.14007					
-0.36416541	-3.52636					
-0.40527947	-3.1209					
-0.34531819	-2.83321					
-0.28878925	-2.42775					
-0.25779235	-2.14007					
-0.73109093	-3.52636	0.0119	0.003115	0.055815897	2.228139	0.124366

-0.49226653	-3.1209
-0.53620754	-2.83321
-0.37132198	-2.42775
-0.39267432	-2.14007
-0.14281672	-1.7346
-0.55941527	-3.52636
-0.44176579	-3.1209
-0.40863257	-2.83321
-0.33655163	-2.42775
-0.24930114	-2.14007
-0.54880598	-3.52636
-0.43983891	-3.1209
-0.52403136	-2.83321
-0.38763354	-2.42775
-0.26273307	-2.14007

0.0246 0.001545 0.039304368 2.776445 0.109126

-0.39124162	-3.52636
-0.34744975	-3.1209
-0.32557367	-2.83321
-0.25072024	-2.42775
-0.15260075	-2.14007
-0.0814388	-1.7346
-0.32873523	-3.52636
-0.34864629	-3.1209
-0.22903018	-2.83321
-0.24901867	-2.42775
-0.18221477	-2.14007
-0.11470732	-1.7346
-0.39275778	-3.52636
-0.31243568	-3.1209
-0.35023944	-2.83321
-0.26950676	-2.42775
-0.24821981	-2.14007
-0.43001225	-3.52636
-0.31951311	-3.1209
-0.25281172	-2.83321
-0.25767848	-2.42775
-0.15536944	-2.14007
-0.08309807	-1.7346
-0.5297212	-3.52636
-0.54798448	-3.1209
-0.40329053	-2.83321
-0.31737632	-2.42775

0.0114 0.001535 0.039182669 2.200985 0.08624

0.0119 0.001582 0.039771442 2.228139 0.088616

0.0061 0.000685 0.026176973 2.093024 0.054789

-0.24575281	-2.14007
-0.56352216	-3.52636
-0.45953428	-3.1209
-0.4571048	-2.83321
-0.41138613	-2.42775
-0.28047106	-2.14007
-0.5196885	-3.52636
-0.43693518	-3.1209
-0.45843412	-2.83321
-0.39407265	-2.42775
-0.31930518	-2.14007
-0.57333894	-3.52636
-0.51697359	-3.1209
-0.46724874	-2.83321
-0.37621313	-2.42775
-0.30143764	-2.14007